Okada Y Watanabe M Nakai T Kamikawa Y Shimizu M Fukuhara Y Yonekura M Matsuura E Hoshika Y Nagai R Aird WC Doi	RUNX1, but not its familial platelet disorder mutants, synergistically activates PF4 gene expression in combination with ETS family proteins.	*J Thromb Haemost.*	9	1742–1750	2013

A Baculoviral Display System to Assay Viral Entry

Manami Iida,[a,#] Takeshi Yoshida,[a,#] Akihiro Watari,[a] Kiyohito Yagi,[a] Takao Hamakubo,[b] and Masuo Kondoh*[,a]

[a] *Laboratory of Bio-Functional Molecular Chemistry, Graduate School of Pharmaceutical Sciences, Osaka University; Suita, Osaka 565–0871, Japan: and* [b] *Department of Quantitative Biology and Medicine, Research Center for Advanced Science and Technology, The University of Tokyo; Tokyo 153–8904, Japan.*

Received August 9, 2013; accepted August 22, 2013

In this study, we evaluated a baculoviral display system for analysis of viral entry by using a recombinant adenovirus (Ad) carrying a luciferase gene and budded baculovirus (BV) that displays the adenoviral receptor, coxsackievirus and adenovirus receptor (CAR). CAR-expressing B16 cells (B16-CAR cells) were infected with luciferase-expressing Ad vector in the presence of BV that expressed or lacked CAR (CAR-BV and mock-BV, respectively). Treatment with mock-BV even at doses as high as 5 μg/mL failed to attenuate the luciferase activity of B16-CAR cells. In contrast, treatment with CAR-BV with doses as low as 0.5 μg/mL significantly decreased the luciferase activity of infected cells, which reached 65% reduction at 5 μg/mL. These findings suggest that a receptor-displaying BV system could be used to evaluate viral infection.

Key words baculovirus; virus; infection; receptor

The process of viral infection involves entry of the virus into the cell, followed by replication of the viral genome and other viral components in the host cell.[1)] Whereas the molecular mechanisms underlying viral replication have largely been elucidated, the key molecules for entry, the viral receptors on host cells, have never been fully identified. Most host receptors are integral membrane proteins, and it is difficult to prepare their recombinant proteins because of their hydrophobicity. Since recombinant proteins are needed to screen inhibitors for viral entry and to produce antibodies against host receptors, preparation of inhibitors, such as chemicals, peptides and antibodies, for viral entry has been delayed.

The baculoviral expression system in insect cells has been widely used for preparation of recombinant proteins.[2)] Hamakubo and colleagues found that baculoviral particles are released from baculovirus-infected cells; the membranes of these budded baculovirus (BV) display host-cell-derived membrane proteins.[3)] Interestingly, the activity and topology of these host-origin proteins remain intact in the baculoviral membrane.[4)] Moreover, a baculoviral envelope protein gp64 trasngenic mice were generated, and method to generate monoclonal antibodies against membrane proteins by immunization of gp64 transgenic mice with membrane protein-displayed baculovirus has been established.[5)] These findings suggest that a baculoviral display system may be useful for assaying viral entry, leading to creation of monoclonal antibodies against host receptors.

In the present study, we investigated whether a baculoviral display system work as an assay system for viral entry using recombinant adenovirus (Ad) vector and a receptor for Ad, coxsackievirus and adenovirus receptor (CAR).[6)]

MATERIALS AND METHODS

Cell Culture Mouse melanoma B16-CAR cells[7)] were cultured in Dulbecco's modified Eagle's medium (DMEM) supplemented with 10% fetal calf serum (FCS) and 2 mg/mL G418. 293 cells were cultured in DMEM supplemented with 10% FCS. Sf9 cells (Invitrogen, Gaithersburg, MD, U.S.A.) were cultured in Grace's insect cell culture medium supplemented with 10% FCS.

Preparation of Recombinant Ad Vector An improved *in vitro* ligation method[8)] was used to generate a recombinant type 5 Ad vector that encoded a fusion protein comprising enhanced green fluorescence protein and firefly luciferase (EGFPLuc). The recombinant Ad vector (Ad-EGFPLuc) was purified from transfected cells by using $CsCl_2$ gradient centrifugation. Viral titers were determined spectrophotometrically.[9)]

Preparation of Recombinant Baculoviruses Recombinant BVs were prepared by using the Bac-to-Bac Baculovirus Expression System (Invitrogen) according to the manufacturer's protocol. Sf9 cells were transduced with the CAR-encoding bacmid, recombinant CAR-BV were recovered by centrifugation of the conditioned medium,[10)] and Sf9 cells were infected with recombinant CAR-BV. At 72 h after infection, the culture supernatant of the infected Sf9 cells was centrifuged to pellet recombinant CAR-BV, which were resuspended in Tris-buffered saline and stored at 4°C until use.

Western Blotting Mock-BV, CAR-BV, and B16-CAR cells were lysed in lysis buffer (25 mM Tris–HCl [pH 7.5], 1% Triton X-100, 0.5% sodium deoxycholate, 150 mM NaCl, 5 mM ethylenediaminetetraacetic acid (EDTA)) containing protease inhibitors (Sigma, St. Louis, MO, U.S.A.). The protein content of the resulting lysates was measured by using the BCA protein assay kit (Pierce Chemical, Rockford, IL, U.S.A.), with bovine serum albumin as the standard. Samples of cellular lysates (20 μg) and BV lysates (5 μg) underwent sodium dodecyl sulfate–polyacrylamide gel electrophoresis followed by blotting of proteins to a polyvinylidene difluoride membrane. The membrane was treated with 5% skim milk to inhibit nonspecific binding, incubated with an anti-goat CAR antibody (R&D Systems, Minneapolis, MN, U.S.A.), and then incubated with a peroxidase-labeled secondary antibody. Immunoreactive bands were visualized by using chemiluminescence reagents (GE Healthcare, Buckinghamshire, U.K.).

Infection Assay Aliquots of Ad-EGFPLuc vector (4×10^7

The authors declare no conflict of interest.

[#] These authors contributed equally to this work.

* To whom correspondence should be addressed. e-mail: masuo@phs.osaka-u.ac.jp

viral particles per mL) were incubated with mock-BV or CAR-BV (0.5 or 5 μg/mL) and an anti-BV gp64 antibody (0.065 or 0.65 μg/mL; AcV1, Santa Cruz Biotechnology, CA, U.S.A.) for 2 h at 37°C to prevent non-specific binding of gp64 to cells. B16-CAR cells were seeded onto 96-well plates (2×10^4 cells per well); 50 μL of the mixture of Ad vector and BVs was added to each well and incubated for 15 min, after which the medium was replaced with fresh growth medium. After an additional 24 h of culture, the luciferase activity in the lysates was measured by using a luminometer.

Statistical Analysis The data were analyzed for statistical significance by Student's *t*-test.

RESULTS AND DISCUSSION

First, we prepared CAR-displaying BV. Lysates of CAR-B16 cells, a mouse myeloma line that expresses mouse CAR, yielded two bands, at 40 and 46 kDa (Fig. 1). In contrast, lysates of CAR-BV showed not only the 40-kDa form but also several bands lower and upper than 40 kDa (Fig. 1); these bands likely represent post-translational modifications. CAR contains two *N*-glycosylation sites and two disulfide-bonded loops in the extracellular domain. The putative molecular sizes of CAR are 40 and 46 kDa, in its non-glycosylated form and glycosylated forms, respectively.[6] Protein folding and post-translational processing, particularly *N*-glycosylation, in insect cells differs markedly from that in mammal cells.[11–13] For example, prolactin receptor expressed in insect cells was 29 kDa larger than that expressed in mammalian cells; this difference was attributed to *N*-glycosylation and ubiquitination.[14]

To investigate whether CAR-BV inhibited adenoviral entry, B16-CAR cells were infected with Ad vector expressing luciferase in the presence of mock-BV or CAR-BV. Whereas treatment with mock-BV at doses as high as 5 μg/mL did not attenuate the luciferase activity of the infected B16-CAR cells, treatment with as little as 0.5 μg/mL CAR-BV significantly decreased their luciferase activity, which reaching 65% reduction at 5 μg/mL (Fig. 2). These findings indicate that CAR-BV prevented the infection of cells by Ad vector. In support of our finding, recombinant prolactin receptor expressed in insect cells and prolactin receptor purified from rabbit mammary gland showed similar specificity and affinity to prolactin.[14] Accordingly, the post-translational modification of CAR in insect cells may not hamper the ability of Ad vector to bind to its receptor.

Our current findings suggest that a baculoviral display system may be useful in the analysis of viral infection, which involves binding of the viral envelope to the viral receptor in the membrane of the host cell. Baculoviral display systems have also been used widely to generate monoclonal antibodies against the extracellular regions of membrane proteins.[3,15] Future applications of baculoviral display systems might contribute the analysis of the mechanisms underlying the entry of pathogens into host cells and the generation of inhibitors of viral entry.

Acknowledgments We thank Prof. H. Mizuguchi (Osaka University) and the members of our laboratory for providing us CAR cDNA and CAR-expressing B16 cells, and useful comments, respectively. This work was supported by a Grant-in-Aid for Scientific Research from the Ministry of Education, Culture, Sports, Science and Technology of Japan (24390042), by a Health and Labour Sciences Research Grant from the Ministry of Health, Labor, and Welfare of Japan, the Takeda Science Foundation and the Nakatomi Foundation.

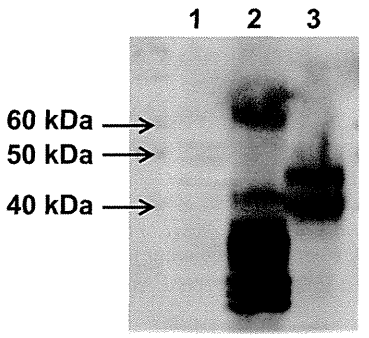

Fig. 1. Preparation of CAR-Displaying BV

Lysates of mock-BV (5 μg, lane 1), CAR-BV (5 μg, lane 2), and CAR-B16 cells (20 μg, lane 3) underwent Western blotting by using a polyclonal goat anti-CAR antibody and a peroxidase-labeled secondary antibody. The arrows indicate the positions of marker proteins.

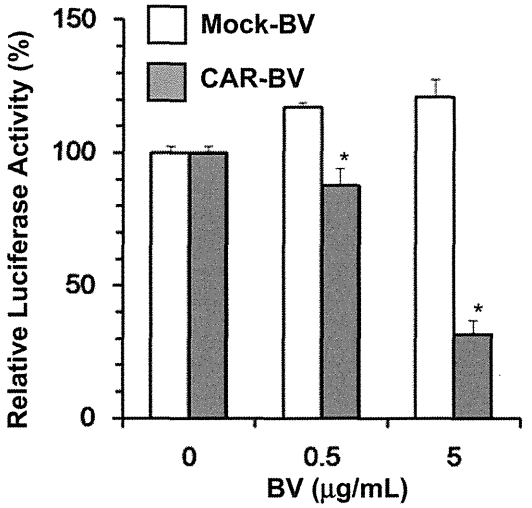

Fig. 2. Effects of CAR-Displaying BV on Ad Vector Infection

Ad vectors (4×10^7 viral particles per mL) were incubated with mock-BV or CAR-BV at 0, 0.5, or 5 μg/mL for 2 h at 37°C. B16-CAR cells were exposed to the Ad–BV mixtures, cultured for 24 h in fresh medium, lysed, and evaluated for luciferase activity. Data are given as luciferase activity relative to that of cells not exposed to BV. Data are shown as mean±S.D. (n=3). *Significant difference compared with mock-BV ($p<0.05$).

REFERENCES

1) Cosset FL, Lavillette D. Cell entry of enveloped viruses. *Adv. Genet.*, **73**, 121–183 (2011).
2) Bieniossek C, Imasaki T, Takagi Y, Berger I. MultiBac: expanding the research toolbox for multiprotein complexes. *Trends Biochem. Sci.*, **37**, 49–57 (2012).
3) Tanaka T, Takeno T, Watanabe Y, Uchiyama Y, Murakami T, Yamashita H, Suzuki A, Aoi R, Iwanari H, Jiang SY, Naito M, Tachibana K, Doi T, Shulman AI, Mangelsdorf DJ, Reiter R, Auwerx J, Hamakubo T, Kodama T. The generation of monoclonal antibodies against human peroxisome proliferator-activated receptors (PPARs). *J. Atheroscler. Thromb.*, **9**, 233–242 (2002).
4) Sakihama T, Masuda K, Sato T, Doi T, Kodama T, Hamakubo T. Functional reconstitution of G-protein-coupled receptor-mediated adenylyl cyclase activation by a baculoviral co-display system. *J.*

Biotechnol., **135**, 28–33 (2008).
5) Saitoh R, Ohtomo T, Yamada Y, Kodama N, Nezu J, Kimura N, Funahashi S, Furugaki K, Yoshino T, Kawase Y, Kato A, Ueda O, Jishage K, Suzuki M, Fukuda R, Arai M, Iwanari H, Takahashi K, Sakihama T, Ohizumi I, Kodama T, Tsuchiya M, Hamakubo T. Viral envelope protein gp64 transgenic mouse facilitates the generation of monoclonal antibodies against exogenous membrane proteins displayed on baculovirus. *J. Immunol. Methods*, **322**, 104–117 (2007).
6) Arnberg N. Adenovirus receptors: implications for targeting of viral vectors. *Trends Pharmacol. Sci.*, **33**, 442–448 (2012).
7) Yamashita M, Ino A, Kawabata K, Sakurai F, Mizuguchi H. Expression of coxsackie and adenovirus receptor reduces the lung metastatic potential of murine tumor cells. *Int. J. Cancer*, **121**, 1690–1696 (2007).
8) Mizuguchi H, Kay MA. A simple method for constructing E1- and E1/E4-deleted recombinant adenoviral vectors. *Hum. Gene Ther.*, **10**, 2013–2017 (1999).
9) Maizel JV Jr, White DO, Scharff MD. The polypeptides of adenovirus. I. Evidence for multiple protein components in the virion and a comparison of types 2, 7A, and 12. *Virology*, **36**, 115–125 (1968).
10) Saeki R, Kondoh M, Kakutani H, Tsunoda S, Mochizuki Y, Hamakubo T, Tsutsumi Y, Horiguchi Y, Yagi K. A novel tumor-targeted therapy using a claudin-4-targeting molecule. *Mol. Pharmacol.*, **76**, 918–926 (2009).
11) Altmann F, Staudacher E, Wilson IB, Marz L. Insect cells as hosts for the expression of recombinant glycoproteins. *Glycoconj. J.*, **16**, 109–123 (1999).
12) Voss T, Ergulen E, Ahorn H, Kubelka V, Sugiyama K, Maurer-Fogy I, Glossl J. Expression of human interferon omega 1 in Sf9 cells. No evidence for complex-type *N*-linked glycosylation or sialylation. *Eur. J. Biochem.*, **217**, 913–919 (1993).
13) Yeh JC, Seals JR, Murphy CI, van Halbeek H, Cummings RD. Site-specific *N*-glycosylation and oligosaccharide structures of recombinant HIV-1 gp120 derived from a baculovirus expression system. *Biochemistry*, **32**, 11087–11099 (1993).
14) Cahoreau C, Petridou B, Cerutti M, Djiane J, Devauchelle G. Expression of the full-length rabbit prolactin receptor and its specific domains in baculovirus infected insect cells. *Biochimie*, **74**, 1053–1065 (1992).
15) Hayashi I, Takatori S, Urano Y, Miyake Y, Takagi J, Sakata-Yanagimoto M, Iwanari H, Osawa S, Morohashi Y, Li T, Wong PC, Chiba S, Kodama T, Hamakubo T, Tomita T, Iwatsubo T. Neutralization of the gamma-secretase activity by monoclonal antibody against extracellular domain of nicastrin. *Oncogene*, **31**, 787–798 (2012).

European Journal of Pharmaceutical Sciences 52 (2014) 132–137

Contents lists available at ScienceDirect

European Journal of Pharmaceutical Sciences

journal homepage: www.elsevier.com/locate/ejps

Tissue distribution and safety evaluation of a claudin-targeting molecule, the C-terminal fragment of *Clostridium perfringens* enterotoxin

Xiangru Li, Rie Saeki, Akihiro Watari, Kiyohito Yagi, Masuo Kondoh *

Laboratory of Bio-Functional Molecular Chemistry, Graduate School of Pharmaceutical Sciences, Osaka University, Suita, Osaka 565-0871, Japan

ARTICLE INFO

Article history:
Received 2 April 2013
Received in revised form 25 October 2013
Accepted 25 October 2013
Available online 11 November 2013

Keywords:
Claudin
Clostridium perfringens enterotoxin
Kidney
Liver
Tissue distribution

ABSTRACT

We previously found that claudin (CL) is a potent target for cancer therapy using a CL-3 and -4-targeting molecule, namely the C-terminal fragment of *Clostridium perfringens* enterotoxin (C-CPE). Although CL-3 and -4 are expressed in various normal tissues, the safety of this CL-targeting strategy has never been investigated. Here, we evaluated the tissue distribution of C-CPE in mice. Ten minutes after intravenous injection into mice, C-CPE was distributed to the liver and kidney (24.0% and 9.5% of the injected dose, respectively). The hepatic level gradually fell to 3.2% of the injected dose by 3 h post-injection, whereas the renal C-CPE level gradually rose to 46.5% of the injected dose by 6 h post-injection and then decreased. A C-CPE mutant protein lacking the ability to bind CL accumulated in the liver to a much lesser extent (2.0% of the dose at 10 min post-injection) than did C-CPE, but its renal profile was similar to that of C-CPE. To investigate the acute toxicity of CL-targeted toxin, we intravenously administered C-CPE-fused protein synthesis inhibitory factor to mice. The CL-targeted toxin dose-dependently increased the levels of serum biomarkers of liver injury, but not of kidney injury. Histological examination confirmed that injection of CL-targeted toxin injured the liver but not the kidney. These results indicate that potential adverse hepatic effects should be considered in C-CPE-based cancer therapy.

1. Introduction

Most lethal cancers are derived from epithelial tissues (Jemal et al., 2008), and many therapeutic strategies targeting such cancers have been developed. Selective delivery of anti-cancer agents to cancer cells is a popular anti-cancer strategy (Adair et al., 2012; Yewale et al., 2013). Many membrane proteins that are present at much higher levels in cancer cells than in normal cells have been identified. Antibodies have recently become available as anti-cancer drugs targeting breast cancer (pertuzumab, directed against human epidermal growth factor receptor-2) and colon cancer (panitumumab, directed against epidermal growth factor receptor) (Dent et al., 2013; Zouhairi et al., 2011).

Normal epithelial cells develop complex intercellular tight junctions (TJs) that prevent the free movement of solutes across epithelial cell sheets and of membrane proteins and lipids between apical and basolateral membranes (Furuse and Tsukita, 2006; Rodriguez-Boulan and Nelson, 1989; Vermeer et al., 2003). In contrast, TJ functionality is frequently abnormal in transformed epithelial cells. As a result, cellular polarity and intercellular contact are often lost, both in the early stages of carcinogenesis and in advanced tumors (Wodarz and Nathke, 2007). Such findings indicate that the membrane proteins of TJs, which are difficult to access in normal epithelia but are exposed in malignant cells, may be candidate targets for cancer therapy.

Freeze-fracture replica electron microscopy has shown that TJs present as a series of continuous, anastomotic, intramembranous particulate strands, or fibrils (Farquhar and Palade, 1963; Staehelin, 1973). The TJ-containing strands are composed of both intracellular and integral membrane proteins, including claudin (CL) (Anderson and Van Itallie, 2009). CL comprises a tetraspan protein family with 27 members (Mineta et al., 2011). Interestingly, the expression of CL-3 or -4, or both, is increased in breast, gastric, intestinal, ovarian, pancreatic, and prostatic carcinomas (Singh et al., 2010; Tsukita et al., 2008; Turksen and Troy, 2011).

Clostridium perfringens enterotoxin (CPE) causes food poisoning in humans (McClane and Chakrabarti, 2004). CL-3 and CL-4 serve as receptors for CPE, and CPE is cytotoxic to cells expressing these CLs (Long et al., 2001; Sonoda et al., 1999). Intratumoral administration of CPE attenuates pancreatic tumor growth, and intraperitoneal administration of CPE inhibits ovarian tumor growth

Abbreviations: ALT, alanine aminotransferase; AST, aspartate aminotransferase; BSA, bovine serum albumin; BUN, blood urea nitrogen; CL, claudin; CPE, *Clostridium perfringens* enterotoxin; C-CPE, C-terminal fragment of CPE; FACS, fluorescence-activated cell sorter; PBS, phosphate-buffered saline; PSIF, protein synthesis inhibitory factor; TJ, tight junction.

* Corresponding author. Tel.: +81 6 6879 8196; fax: +81 6 6879 8199.
E-mail address: masuo@phs.osaka-u.ac.jp (M. Kondoh).

0928-0987/$ - see front matter © 2013 Elsevier B.V. All rights reserved.
http://dx.doi.org/10.1016/j.ejps.2013.10.018

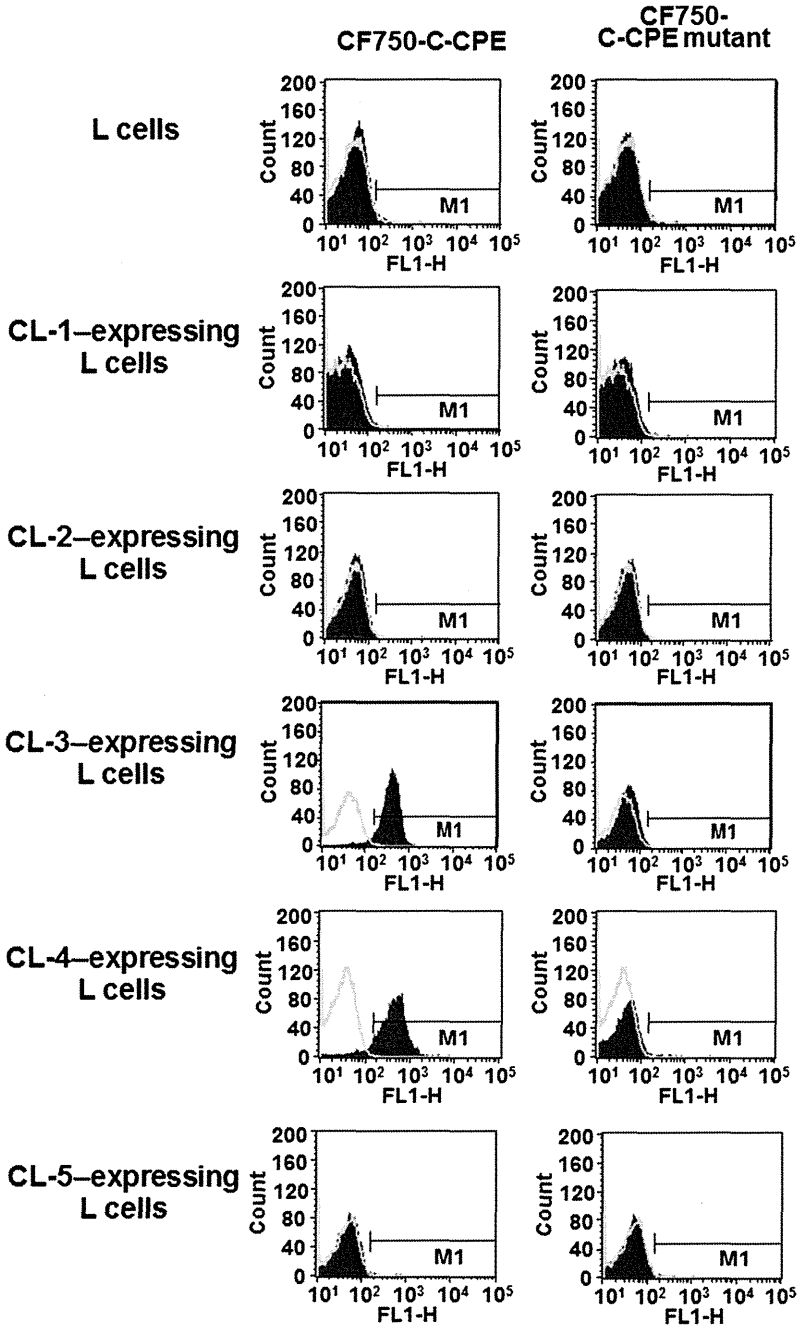

Fig. 1. Flow cytometric analysis of the interaction of claudins (CLs) with the CF750-labeled C-terminal fragment of *Clostridium perfringens* enterotoxin (C-CPE). Mouse fibroblast L cells were incubated with 10 μg/ml CF750-labeled C-CPE or a mutant form of C-CPE (also labeled with CF750) for 1 h and then subjected to fluorescence-activated cell sorter analysis as described in the Materials and Methods. Unfilled curves show the results obtained when cells were not treated with C-CPE proteins. Filled curves show data from C-CPE-treated cells. FL1-H indicates fluorescent intensity and M1 indicates C-CPE-bound cells.

(Michl et al., 2001; Santin et al., 2005). Moreover, the C-terminal fragment of CPE (C-CPE) is a ligand of CL-3 and CL-4 (Sonoda et al., 1999). We previously prepared a CL-targeting cytotoxic molecule via fusion of C-CPE and a protein synthesis inhibitory factor (PSIF) derived from *Pseudomonas* exotoxin (Ebihara et al., 2006). We found that intratumoral or intravenous administration of C-CPE-fused PSIF attenuated the growth of murine breast cancer cells (Saeki et al., 2009, 2010). Thus, drugs that include all or part of CPE may be useful for targeting CLs in cancer therapy.

CLs are expressed throughout the body. Evaluation of the possible adverse effects of CL-targeting molecules is critical if the CPE technology described above is to be used for cancer therapy. However, no such hazard assessment has been performed to date. Here, we investigated the tissue distribution of C-CPE and the tissue injury caused by C-CPE-fused PSIF.

2. Materials and methods

2.1. Cell cultures

Mouse fibroblast L cells expressing mouse CL-1, CL-2, CL-3, CL-4, or CL-5 were kindly provided by Dr. S. Tsukita (Kyoto University). Cells were cultured in Eagle's minimum essential medium with 10% (v/v) fetal calf serum and 500 μg/ml G418 at 37 °C under a 5% (v/v) CO_2 atmosphere.

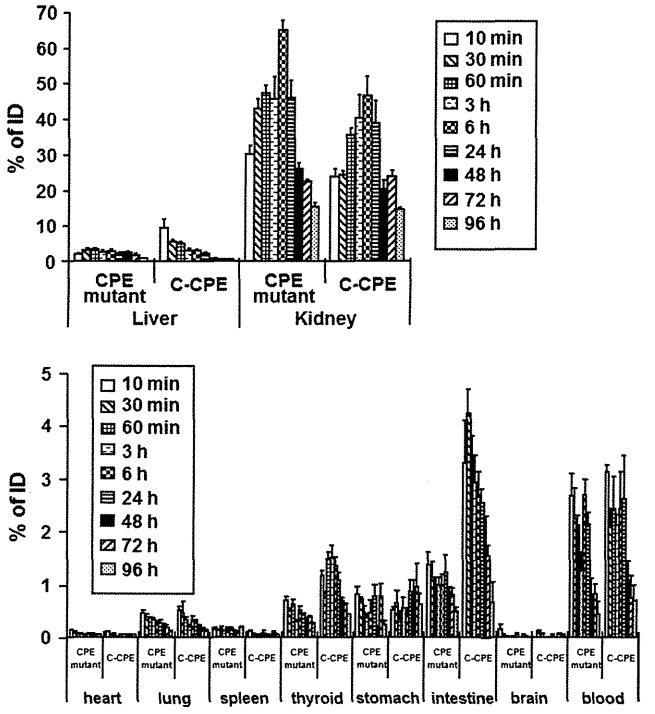

Fig. 2. *In vivo* distribution of the CF750-labeled C-terminal fragment of *Clostridium perfringens* enterotoxin (C-CPE). Mice were intravenously injected with 2 μg/mouse CF750-labeled C-CPE or a CF750-labeled C-CPE mutant. Tissues were removed at the indicated times after injection and the intensity of fluorescence of each tissue was measured as described in the Materials and Methods. Tissue C-CPE levels were calculated as percentages of injected doses. Data are means ± SEM ($n = 5$). ID, injected dose.

2.2. Preparation of C-CPE and C-CPE mutant protein

C-CPE, and a mutant form thereof, in which Ala was substituted with Tyr and Leu at positions 306 and 315, were prepared as described previously (Takahashi et al., 2008). Briefly, recombinant plasmids derived from pET-16b, pET-C-CPE encoding histidine (His)-tagged C-CPE, or a pET-C-CPE mutant encoding His-tagged C-CPE mutant protein, were transduced into *Escherichia coli* strain BL21 (DE3) (Novagen, Darmstadt, Germany), and production of recombinant proteins was induced by adding isopropyl-β-D-thiogalactopyranoside. Harvested cells were lysed in buffer A (10 mM Tris–HCl [pH 8.0], 400 mM NaCl, 5 mM $MgCl_2$, 0.1 mM phenylmethylsulfonyl fluoride, 1 mM 2-mercaptoethanol, and 10% [v/v] glycerol). Each lysate was applied to a HiTrap chelating HP column (GE Healthcare, Chalfont St Giles, Buckinghamshire, UK), and the recombinant protein was eluted with buffer A containing imidazole. This buffer was exchanged for phosphate-buffered saline (PBS) by using a PD-10 column (GE Healthcare), and the purified proteins dissolved in PBS were stored at −80 °C until use. The purity of the recombinant proteins was confirmed by sodium dodecyl sulfate–polyacrylamide gel electrophoresis followed by staining with Coomassie brilliant blue. Protein concentrations were quantified with a BCA protein assay kit, using bovine serum albumin (BSA) as a standard (Pierce Chemicals, Rockford, IL).

2.3. Animals

Female BALB/c mice (6–8 weeks of age) were purchased from SLC, Inc. (Shizuoka, Japan). Mice were housed at 23 ± 1.5 °C with a 12-h light/12-h dark cycle and had free access to water and commercial chow (Type MF; Oriental Yeast, Tokyo, Japan). Mice were allowed to adapt to these conditions for at least 1 week after arrival. All animal experiments adhered to the ethical guidelines of the Graduate School of Pharmaceutical Sciences, Osaka University.

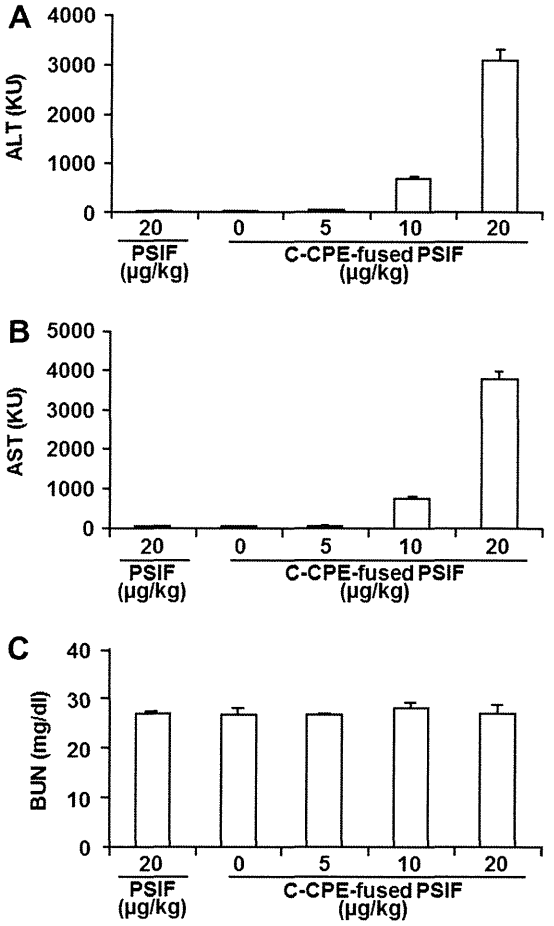

Fig. 3. Serum markers of liver and kidney injury in mice injected with protein synthesis inhibitory factor (PSIF) fused to the C-terminal fragment of *Clostridium perfringens* enterotoxin (C-CPE). Mice were intravenously injected with PSIF at 2 μg/kg or C-CPE-fused PSIF at 0, 5, 10, or 20 μg/kg. Twenty-four hours later, serum ALT (A), AST (B), and BUN (C) levels were measured as described in the Materials and Methods. Data are presented as means ± SEM ($n = 5$).

2.4. Preparation of CF750-labeled C-CPE proteins

C-CPE and the mutant form of the protein were labeled with the fluorescent dye CF750 by using a XenoLight CF750 rapid antibody-labeling kit (Caliper Life Sciences, Inc., Hopkinton, MA), in accordance with the manufacturer's instructions. The concentrations of labeled C-CPEs were calculated according to the manufacturer's protocol by using the following equation: Concentration (mg/ml) = {[absorbance at 280 nm minus (absorbance at 755 nm × 0.3)]/0.46} × dilution factor.

2.5. Fluorescence-activated cell sorter (FACS) analysis

L-cells expressing various CLs were harvested with trypsin and suspended in PBS. The cells were incubated with C-CPE or the mutant form of C-CPE for 1 h at 4 °C; this was followed by incubation with anti-His-tag antibody. Cells were next incubated with fluorescein-labeled secondary antibody, and cells that bound the test proteins were detected and analyzed by flow cytometry (FACScalibur, Becton Dickinson, Franklin Lakes, NJ).

2.6. Tissue distribution of injected proteins

C-CPE, or the mutant form thereof, labeled with CF750, was intravenously injected into mice at 2 μg/100 μl of PBS per mouse. Mice were sacrificed 10 min, 30 min, 60 min, 3 h, 6 h, 24 h, 48 h,

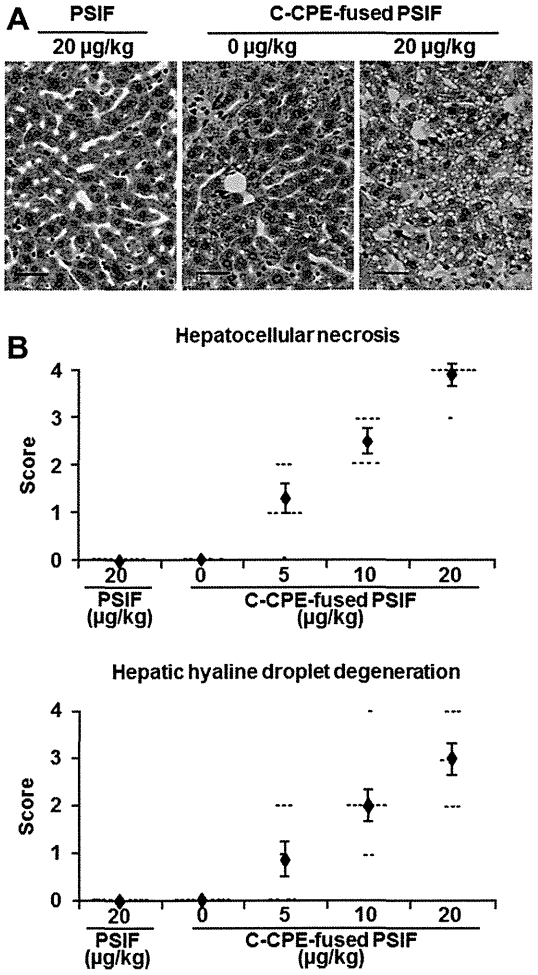

Fig. 4. Histological analysis of the livers of mice injected with protein synthesis inhibitory factor (PSIF) fused to the C-terminal fragment of *Clostridium perfringens* enterotoxin (C-CPE). Mice were intravenously injected with PSIF at 20 μg/kg or C-CPE-fused PSIF at 0, 5, 10, or 20 μg/kg (n = 7 or 8). Twenty-four hours later, the livers were removed and fixed in formaldehyde. Sections were stained with hematoxylin–eosin and examined microscopically for pathology. A representative micrograph is shown in panel A; arrows indicate regions of injury (scale bar, 60 μm). The extents of hepatocellular necrosis and hepatic hyaline droplet degeneration were scored (panel B) as follows: 0, none; 1, very mild; 2, mild; 3, moderate; or 4, high. Each horizontal dash represents the score of one sample. Data are means ± SEM (n = 7 or 8).

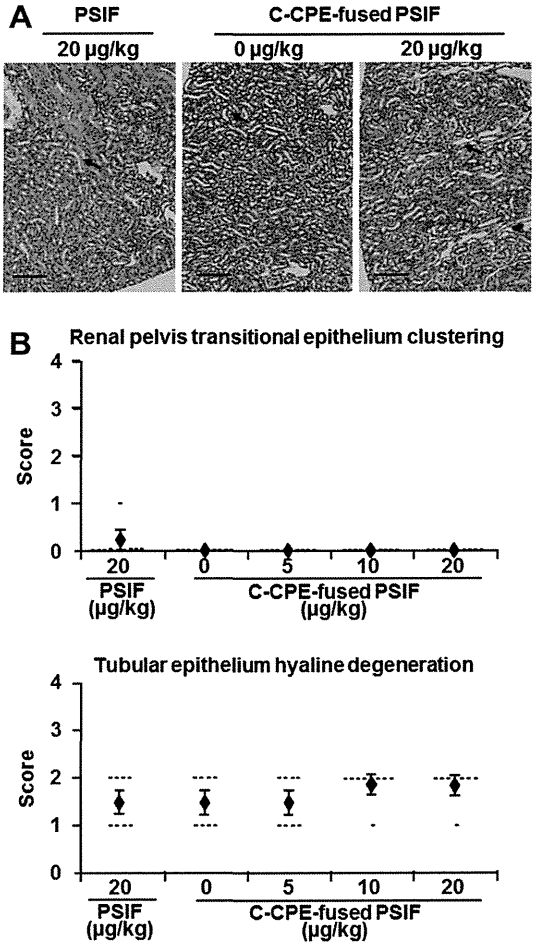

Fig. 5. Histological analysis of the kidneys of mice injected with protein synthesis inhibitory factor (PSIF) fused to the C-terminal fragment of *Clostridium perfringens* enterotoxin (C-CPE). Mice were intravenously injected with PSIF at 20 μg/kg or C-CPE-fused PSIF at 0, 5, 10, or 20 μg/kg (n = 7 or 8). Twenty-four hours later, the kidneys were removed and fixed in formaldehyde. Sections were stained with hematoxylin-eosin and examined microscopically for pathology. A representative micrograph is shown in panel A; arrows indicate regions of injury (scale bar, 240 μm). The extent of clustering of the renal pelvis transitional epithelium and the level of hyaline degeneration of the tubular epithelium were scored (panel B) as follows: 0, none; 1, very mild; 2, mild; 3, moderate; or 4, high. Each horizontal dash represents the score of one sample. Data are means ± SEM (n = 7 or 8).

72 h, or 96 h later. The blood, heart, lung, liver, spleen, kidney, thyroid, stomach, intestine, and brain were excised from each mouse. The blood and organs from each mouse were placed side-by-side and imaged by using a Maestro EX *in vivo* imaging system, version 2.10.0 (Cambridge Research & Instrumentation Inc., Woburn, MA). The imaging system was equipped with an excitation filter (wavelength 229–684 nm). Fluorescence was detected by a CCD camera equipped with a C-mount lens and a long-pass emission filter (745 nm). Spectral data "cubes" were created by acquisition of a series of images obtained by using different wavelengths. In such cubes, each pixel is associated with a spectrum. Maestro software can be used to analyze these data; any autofluorescence can be identified, separated from the CF750 fluorescence, and removed. The resulting signals (counts) from each tissue were used to evaluate C-CPE distributions. The levels of C-CPEs in each tissue, as percentages of injected doses, were calculated. Total blood volume was calculated as 8% of body weight.

2.7. Preparation of C-CPE-fused PSIF

PSIF and C-CPE-fused PSIF were prepared as described previously (Saeki et al., 2009). In brief, plasmid pET-PSIF or pET-C-CPE-PSIF was transduced into *E. coli* BL21 (DE3) and recombinant protein production was induced by adding 0.25 mM isopropyl-β-D-thiogalactopyranoside. Harvested cells were lysed in buffer A. The lysates were centrifuged and the supernatants applied to Hi-Trap chelating HP columns. Recombinant proteins were eluted with imidazole-containing buffer A. This buffer was exchanged for PBS by using a PD-10 column, and the purified protein solutions were stored at −80 °C until use. Protein concentrations were quantified with a BCA protein assay kit, using BSA as a standard.

2.8. Biochemical assays

Mice were intravenously injected with 100 μl of C-CPE-fused PSIF at 0, 5, 10, or 20 μg/kg, or with 100 μl of PSIF at 20 μg/kg.

Twenty-four hours after the injection, serum levels of alanine aminotransferase (ALT), aspartate aminotransferase (AST), and blood urea nitrogen (BUN) were measured with commercial kits (Transaminase-CII kit [ALT, AST] and Blood Urea Nitrogen-B Test [BUN]; Wako Pure Chemicals, Osaka, Japan).

2.9. Histological analysis

Livers and kidneys were removed and fixed in 4% (v/v) paraformaldehyde. Thin sections were stained with hematoxylin and eosin before histological observation. The extent of injury was scored as 0, none; 1, very mild; 2, mild; 3, moderate; or 4, high.

3. Results

3.1. Tissue distribution of the CL-3/-4-binding agent C-CPE

The fluorescent dye CF750 was conjugated to the CL-3/-4-binding agent C-CPE to allow the tissue distribution of C-CPE to be monitored. FACS analysis revealed that CF750-labeled C-CPE bound to CL-3- or CL-4-expressing L-cells but not to mock-, CL-1-, CL-2-, or CL-5-expressing L cells (Fig. 1). Thus, labeling of C-CPE with CF750 did not affect the binding profile of C-CPE to CLs. As a control, we also prepared a CF750-labeled C-CPE mutant protein lacking CL-binding activity; Ala was substituted for the wild-type Tyr306 and Leu315 in the mutant protein (Takahashi et al., 2008). The C-CPE mutant did not bind to the cells (Fig. 1).

C-CPE was evident in the kidney (24.0% of the injected dose), liver (9.5%), intestine (3.3%), and thyroid (1.2%) 10 min after intravenous injection (Fig. 2). The levels of C-CPE in the liver, intestine, and thyroid gradually fell thereafter, to 0.4%, 0.7%, and 0.4% of the injected dose, respectively, at 96 h post-injection. In contrast, the level of C-CPE in the kidney increased to 46.5% of the injected dose 6 h after injection and only then began to fall, reaching 14.4% of the injected dose 96 h post-injection. The control C-CPE mutant protein became distributed in the liver (2.0% of the injected dose), intestine (1.4%), and thyroid (0.7%) at levels much lower than those of C-CPE at 10 min post-injection, but the levels of the mutant protein in the kidney were comparable to those of C-CPE (Fig. 2). Therefore, the liver may be a major target tissue of CL-3/-4-binding protein, whereas accumulation in the kidney may not be associated with CL-3/-4 targeting.

3.2. Effects of a CL-3/-4-targeting toxin on the liver and kidney

We previously found that tail vein injection of C-CPE-fused PSIF at 5 μg/kg every 2 days for 14 days had anti-tumor activity without hepatotoxicity or nephrotoxicity (Saeki et al., 2010). Here, to evaluate the acute toxicity of a CL-targeting toxin to the liver and kidney, we intravenously injected mice with C-CPE-fused PSIF, or control PSIF alone, and measured biochemical markers of liver (ALT and AST) and kidney (BUN) injury 24-h later. Injection of PSIF alone (20 μg/kg) did not increase serum ALT, AST, or BUN levels. Injection of C-CPE-fused PSIF at doses of 0, 5, 10, and 20 μg/kg increased serum ALT and AST levels in a dose-dependent manner (ALT: 21, 49, 668, and 3053 karmen unit (KU) respectively; AST: 49, 68, 764, and 3781 KU, respectively) (Fig. 3A and B). In contrast, injection of C-CPE-fused PSIF, even at 20 μg/kg, did not increase the serum BUN level (Fig. 3C). Injection of C-CPE-fused PSIF at 10 or 20 μg/kg, but not at 5 μg/kg, caused body weight loss and reduced mobility (data not shown). Histologically, C-CPE-fused PSIF caused hepatocellular necrosis and hyaline droplet degeneration (Fig. 4A, B). Although injection of C-CPE-fused PSIF caused slight hyaline degeneration of the tubular epithelium of the kidney, injection of PSIF alone had a similar effect (Fig. 5A and B). Therefore, the low-level kidney injury evident after administration of C-CPE-fused PSIF may not have been associated with the targeting of CLs.

4. Discussion

CPE was the first CL-3/-4-targeting toxin to be described (Fujita et al., 2000; Sonoda et al., 1999), and C-CPE-fused PSIF was the second (Ebihara et al., 2006; Saeki et al., 2009). A series of studies using CPE and C-CPE have provided proof-of-concept that CL targeting is a strategy for cancer therapy (Long et al., 2001; Michl et al., 2001; Neesse et al., 2013; Saeki et al., 2009, 2010; Santin et al., 2005). However, because CL-3 and CL-4 are expressed in various normal tissues (Morita et al., 1999; Turksen and Troy, 2011), risk assessment of CL-targeting molecules is needed when CPE technology is applied to cancer therapy. Here, we found that systemic injection of a C-CPE-fused toxin resulted in acute hepatic, but not renal, toxicity 24 h after injection in mice.

After injection, C-CPE accumulates to the greatest extent in the liver and kidney. The expression profiles of CL-3 and CL-4 differ in these two tissues. In the liver, CL-3 is locally expressed in the lateral membranes of all lobular hepatocytes (Rahner et al., 2001); the liver does not express CL-4 (Morita et al., 1999). In contrast, CL-3 and CL-4 are locally expressed, in the kidney, in the lateral membranes of epithelial-cell sheets of the loop of Henle, the distal tubule, and the collecting duct (Balkovetz, 2009). Epithelial cells of the kidney form a boundary between the inner and outer regions, and the TJs act as barriers, preventing free movement of solutes across epithelial sheets (Hou et al., 2010; Milatz et al., 2010). In contrast, hepatocytes do not have a barrier function, with the exception of those located in the canaliculi. Therefore, CL-targeting molecules can access CL-3 in parts of the liver other than the canaliculi, but not CL-3 and CL-4 in the renal epithelium. C-CPE-fused PSIF must be taken up by cells if the drug is to be cytotoxic, because inhibition of ribosomal elongation factor-2 by the PSIF domain is the cause of cell death (Ebihara et al., 2006; Kreitman and Pastan, 2006; Ogata et al., 1990).

Here, we found that hepatic accumulation of a toxin fused to C-CPE could have adverse effects if C-CPE-based cancer therapy were prescribed. C-CPE binds to both CL-3 and CL-4. Levels of CL-4 are increased more frequently than those of CL-3 in cancers such as breast, gastric, intestinal, ovarian, pancreatic, and prostate carcinomas (Singh et al., 2010; Tsukita et al., 2008; Turksen and Troy, 2011). Thus, development of a C-CPE mutant that binds to CL-4 but not to CL-3 may be useful in cancer therapy. We previously found that modulation of the electrostatic profile of the C-CPE surface can change the CL-binding profile (Takahashi et al., 2012). Veshnyakova et al. (2012) showed that the C-CPE residues, Leu223, Asp225, and Arg227, were involved in binding to CL-3, whereas Leu254, Ser256, Ile258, and Asp284 were involved in binding to CL-4. Manipulation of the electrostatic surface and the C-CPE residues may allow us to develop a C-CPE mutant that binds specifically to CL-4.

Acknowledgements

We thank the staff of our laboratory for their useful comments and discussion. This work was supported by Grants-in-Aids for Scientific Research from the Ministry of Education, Culture, Sports, Science, and Technology of Japan (Nos. 21689006 and 24390042); by a Health and Labor Sciences Research Grant from the Ministry of Health, Labour, and Welfare of Japan; by the Takeda Science Foundation; by the Nakatomi Foundation; by the Adaptable and Seamless Technology Transfer Program through Target-driven R&D, Japan Science and Technology Agency; and by the Platform for Drug Discovery, Informatics, and Structural Life Science of the Ministry of Education, Culture, Sports, Science, and Technology, Japan.

References

Adair, J.R., Howard, P.W., Hartley, J.A., Williams, D.G., Chester, K.A., 2012. Antibody-drug conjugates – a perfect synergy. Expert. Opin. Biol. Ther. 12, 1191–1206.

Anderson, J.M., Van Itallie, C.M., 2009. Physiology and function of the tight junction. Cold Spring Harbor Perspect. Biol. 1, a002584.

Balkovetz, D.F., 2009. Tight junction claudins and the kidney in sickness and in health. Biochim. Biophys. Acta 1788, 858–863.

Dent, S., Oyan, B., Honig, A., Mano, M., Howell, S., 2013. HER2-targeted therapy in breast cancer: a systematic review of neoadjuvant trials. Cancer Treat. Rev. 39, 622–631.

Ebihara, C., Kondoh, M., Hasuike, N., Harada, M., Mizuguchi, H., Horiguchi, Y., Fujii, M., Watanabe, Y., 2006. Preparation of a claudin-targeting molecule using a C-terminal fragment of *Clostridium perfringens* enterotoxin. J. Pharmacol. Exp. Ther. 316, 255–260.

Farquhar, M.G., Palade, G.E., 1963. Junctional complexes in various epithelia. J. Cell Biol. 17, 375–412.

Fujita, K., Katahira, J., Horiguchi, Y., Sonoda, N., Furuse, M., Tsukita, S., 2000. *Clostridium perfringens* enterotoxin binds to the second extracellular loop of claudin-3, a tight junction integral membrane protein. FEBS Lett. 476, 258–261.

Furuse, M., Tsukita, S., 2006. Claudins in occluding junctions of humans and flies. Trends Cell Biol. 16, 181–188.

Hou, J., Renigunta, A., Yang, J., Waldegger, S., 2010. Claudin-4 forms paracellular chloride channel in the kidney and requires claudin-8 for tight junction localization. Proc. Natl. Acad. Sci. USA 107, 18010–18015.

Jemal, A., Siegel, R., Ward, E., Hao, Y., Xu, J., Murray, T., Thun, M.J., 2008. Cancer statistics, 2008. CA Cancer J. Clin. 58, 71–96.

Kreitman, R.J., Pastan, I., 2006. Immunotoxins in the treatment of hematologic malignancies. Curr. Drug Targets 7, 1301–1311.

Long, H., Crean, C.D., Lee, W.H., Cummings, O.W., Gabig, T.G., 2001. Expression of *Clostridium perfringens* enterotoxin receptors claudin-3 and claudin-4 in prostate cancer epithelium. Cancer Res. 61, 7878–7881.

McClane, B.A., Chakrabarti, G., 2004. New insights into the cytotoxic mechanisms of *Clostridium perfringens* enterotoxin. Anaerobe 10, 107–114.

Michl, P., Buchholz, M., Rolke, M., Kunsch, S., Lohr, M., McClane, B., Tsukita, S., Leder, G., Adler, G., Gress, T.M., 2001. Claudin-4: a new target for pancreatic cancer treatment using *Clostridium perfringens* enterotoxin. Gastroenterology 121, 678–684.

Milatz, S., Krug, S.M., Rosenthal, R., Gunzel, D., Muller, D., Schulzke, J.D., Amasheh, S., Fromm, M., 2010. Claudin-3 acts as a sealing component of the tight junction for ions of either charge and uncharged solutes. Biochim. Biophys. Acta 1798, 2048–2057.

Mineta, K., Yamamoto, Y., Yamazaki, Y., Tanaka, H., Tada, Y., Saito, K., Tamura, A., Igarashi, M., Endo, T., Takeuchi, K., Tsukita, S., 2011. Predicted expansion of the claudin multigene family. FEBS Lett. 585, 606–612.

Morita, K., Furuse, M., Fujimoto, K., Tsukita, S., 1999. Claudin multigene family encoding four-transmembrane domain protein components of tight junction strands. Proc. Natl. Acad. Sci. USA 96, 511–516.

Neesse, A., Hahnenkamp, A., Griesmann, H., Buchholz, M., Hahn, S.A., Maghnouj, A., Fendrich, V., Ring, J., Sipos, B., Tuveson, D.A., Bremer, C., Gress, T.M., Michl, P., 2013. Claudin-4-targeted optical imaging detects pancreatic cancer and its precursor lesions. Gut 62, 1034–1043.

Ogata, M., Chaudhary, V.K., Pastan, I., FitzGerald, D.J., 1990. Processing of *Pseudomonas* exotoxin by a cellular protease results in the generation of a 37,000-Da toxin fragment that is translocated to the cytosol. J. Biol. Chem. 265, 20678–20685.

Rahner, C., Mitic, L.L., Anderson, J.M., 2001. Heterogeneity in expression and subcellular localization of claudins 2, 3, 4, and 5 in the rat liver, pancreas, and gut. Gastroenterology 120, 411–422.

Rodriguez-Boulan, E., Nelson, W.J., 1989. Morphogenesis of the polarized epithelial cell phenotype. Science 245, 718–725.

Saeki, R., Kondoh, M., Kakutani, H., Tsunoda, S., Mochizuki, Y., Hamakubo, T., Tsutsumi, Y., Horiguchi, Y., Yagi, K., 2009. A novel tumor-targeted therapy using a claudin-4-targeting molecule. Mol. Pharmacol. 76, 918–926.

Saeki, R., Kondoh, M., Kakutani, H., Matsuhisa, K., Takahashi, A., Suzuki, H., Kakamu, Y., Watari, A., Yagi, K., 2010. A claudin-targeting molecule as an inhibitor of tumor metastasis. J. Pharmacol. Exp. Ther. 334, 576–582.

Santin, A.D., Cane, S., Bellone, S., Palmieri, M., Siegel, E.R., Thomas, M., Roman, J.J., Burnett, A., Cannon, M.J., Pecorelli, S., 2005. Treatment of chemotherapy-resistant human ovarian cancer xenografts in C.B-17/SCID mice by intraperitoneal administration of *Clostridium perfringens* enterotoxin. Cancer Res. 65, 4334–4342.

Singh, A.B., Sharma, A., Dhawan, P., 2010. Claudin family of proteins and cancer: an overview. J. Oncol. 2010, 541957.

Sonoda, N., Furuse, M., Sasaki, H., Yonemura, S., Katahira, J., Horiguchi, Y., Tsukita, S., 1999. *Clostridium perfringens* enterotoxin fragment removes specific claudins from tight junction strands: evidence for direct involvement of claudins in tight junction barrier. J. Cell Biol. 147, 195–204.

Staehelin, L.A., 1973. Further observations on the fine structure of freeze-cleaved tight junctions. J. Cell Sci. 13, 763–786.

Takahashi, A., Komiya, E., Kakutani, H., Yoshida, T., Fujii, M., Horiguchi, Y., Mizuguchi, H., Tsutsumi, Y., Tsunoda, S., Koizumi, N., Isoda, K., Yagi, K., Watanabe, Y., Kondoh, M., 2008. Domain mapping of a claudin-4 modulator, the C-terminal region of C-terminal fragment of *Clostridium perfringens* enterotoxin, by site-directed mutagenesis. Biochem. Pharmacol. 75, 1639–1648.

Takahashi, A., Saito, Y., Kondoh, M., Matsushita, K., Krug, S.M., Suzuki, H., Tsujino, H., Li, X., Aoyama, H., Matsuhisa, K., Uno, T., Fromm, M., Hamakubo, T., Yagi, K., 2012. Creation and biochemical analysis of a broad-specific claudin binder. Biomaterials 33, 3464–3474.

Tsukita, S., Yamazaki, Y., Katsuno, T., Tamura, A., Tsukita, S., 2008. Tight junction-based epithelial microenvironment and cell proliferation. Oncogene 27, 6930–6938.

Turksen, K., Troy, T.C., 2011. Junctions gone bad: claudins and loss of the barrier in cancer. Biochim. Biophys. Acta 1816, 73–79.

Vermeer, P.D., Einwalter, L.A., Moninger, T.O., Rokhlina, T., Kern, J.A., Zabner, J., Welsh, M.J., 2003. Segregation of receptor and ligand regulates activation of epithelial growth factor receptor. Nature 422, 322–326.

Veshnyakova, A., Piontek, J., Protze, J., Waziri, N., Heise, I., Krause, G., 2012. Mechanism of *Clostridium perfringens* enterotoxin interaction with claudin-3/-4 protein suggests structural modifications of the toxin to target specific claudins. J. Biol. Chem. 287, 1698–1708.

Wodarz, A., Nathke, I., 2007. Cell polarity in development and cancer. Nat. Cell Biol. 9, 1016–1024.

Yewale, C., Baradia, D., Vhora, I., Misra, A., 2013. Proteins: emerging carrier for delivery of cancer therapeutics. Expert Opin. Drug Deliv. 10, 1429–1448.

Zouhairi, M., Charabaty, A., Pishvaian, M.J., 2011. Molecularly targeted therapy for metastatic colon cancer: proven treatments and promising new agents. Gastrointest. Cancer Res. 4, 15–21.

Current Topics

Challenges of Drug Delivery Systems That Contribute to Cancer Chemotherapy

Recent Advances in Claudin-Targeting Technology

Shotaro Nagase, Ryo Doyama, Kiyohito Yagi, and Masuo Kondoh*

Laboratory of Bio-Functional Molecular Chemistry, Graduate School of Pharmaceutical Sciences, Osaka University; Suita, Osaka 565–0871, Japan.

Received December 31, 2012

Most malignant tumors are derived from epithelium, and pathologic microorganisms often invade the body through the mucosal epithelium. Thus epithelial tissues are potent targets for drug delivery. The tight junction (TJ) is the intercellular seal in epithelial cell sheets. Claudins (CLs) are a family of tetratransmembrane proteins with a molecular mass of approximately 23 kDa. CLs are key structural and sealing components of TJs. CLs are often overexpressed in malignant tumors. CL-4 is highly expressed in the epithelial cells covering mucosal immune tissues. Therefore CLs may be potent targets for drug delivery, cancer therapy, and mucosal vaccination. Herein, we overview a series of our studies using the C-terminal fragment of *Clostridium perfringens* enterotoxin to target and bind CLs; we also discuss the efficacy of CL-targeted drug delivery.

Key words claudin; tight junction; epithelial cell; *Clostridium perfringens* enterotoxin

1. INTRODUCTION

Epithelium plays a pivotal role in protecting the body from various internal and external agents, but sometimes the protective mechanisms of the epithelium can be evaded. For example, most malignant tumors arise from epithelium, and often a very early step in the process of epithelial carcinogenesis is disruption of the cellular polarity of epithelial cells.[1] Consequently, a system that targets depolarized epithelial cells likely will contribute greatly to treating cancer. In addition, the epithelium is the initial physical and immunologic barrier against most pathogens. Using mucosal vaccination to induce immune responses in the mucosal epithelium is a potential key mechanism for preventing infectious diseases.[2] Furthermore, the mucosal epithelium regulates the movement of solutes through intercellular spaces,[3] and strategies to modulate the epithelial barrier for enhancing drug absorption have garnered great interest since the 1960s.[4] In short, epithelial cells are important targets for treating cancer, preventing infectious diseases, and enhancing drug absorption.

Tight junctions (TJs) function as an intercellular seal between epithelial cells. Whereas bicellular TJs contain biochemical complexes including occludin, claudins (CLs), and junctional adhesion molecules,[5] tricellular TJs include at least tricellulin and members of the angulin family.[6–8] Pharmacologic and pathologic research has revealed that CLs offer considerable potential as targets for the delivery of various therapeutic compounds. For instance, CL-1–knockout mice showed increased epidermal permeability to solutes.[9] In addition, local inhibition of CL-1 in peripheral neurons enhanced drug delivery to those cells.[10] Solutes were able to breach the blood–brain barrier of CL-5–deficient mice.[11] Treatment of mucosal epithelium with a CL-4 binder enhanced the absorption of dextran (molecular weight (MW), 4–20 kDa) and a peptide drug (hPTH) across mucosal epithelium.[12,13] The deregulated expression of CLs in malignant tumors makes these proteins potential targets for antineoplastic agents.[14,15] Furthermore, administration of *Clostridium perfringens* enterotoxin (CPE), whose receptor is CL-3 and CL-4, showed antitumor activity.[16–18] Because CL-4 is highly expressed in the epithelium covering mucosal immune tissues, the delivery of antigen to these tissues using a CL-4 ligand may lead to the development of mucosal vaccines.[19] Therefore CLs are very attractive as targets for drug delivery. However, the hydrophobicity and low immunogenicity of CLs have made it difficult to prepare CL binders, including antibodies, and have delayed the development of CL-targeted drug delivery systems.

Herein, we provide an overview of our efforts to develop CL binders for applications in antitumor therapy and mucosal vaccines.

2. TARGETING CANCER

Most lethal cancers are derived from epithelial tissues.[20] Malignant tumor cells frequently exhibit abnormal TJ functions, followed by deregulation of cellular polarity and intercellular contact—features that are common to both early carcinogenesis and advanced tumors.[1] In addition, CLs are key components of TJs, and some CLs are overexpressed in various types of cancers. For example, CL-4 expression frequently is upregulated in breast, prostate, pancreatic, and ovarian cancers.[15] Although typically nearly inaccessible in well-differentiated normal epithelia, CLs are fairly exposed on malignant tumor cells and therefore may be promising candidates for cancer-targeted therapy.

To investigate whether a CL-targeted strategy offers hope as a cancer-targeting mechanism, we generated a fusion protein that combined C-CPE (the C-terminal fragment of

The authors declare no conflict of interest.

* To whom correspondence should be addressed. e-mail: masuo@phs.osaka-u.ac.jp

CPE), a CL-4 binder, with protein synthesis inhibitory factor (PSIF).[21,22] PSIF has been widely used for tumor-targeting therapy[23,24] but it cannot enter cells on its own. Whereas neither C-CPE nor PSIF alone led to cytotoxicity, our C-CPE–fused PSIF dose-dependently killed CL-4–expressing L cells, reaching >90% cell death at 10 ng/mL; in contrast, C-CPE–fused PSIF showed no cytotoxicity of CL-1, -2, or -5–expressing L cells.[22] To confirm the CL-specificity of C-CPE–PSIF in other cell lines, we tested C-CPE–PSIF in CL-4–positive HepG2 cells and CL-4–negative SK-HEP-1 cells. Whereas C-CPE–PSIF was toxic to HepG2 cells at doses as low as 1 ng/mL, the fusion protein had no effect on SK-HEP-1 cells, even at doses as high as 100 ng/mL.[22] These results indicate that C-CPE–PSIF may be an effective CL-4–targeting cytotoxic agent.

CL-4 is expressed in various tissues, including lung, intestine, liver, and kidney. In normal healthy cells CLs predominantly remain sequestered in TJ complexes, but this localization of CLs is deregulated in some cancers.[14,15] To investigate whether C-CPE–PSIF can recognize the deregulated localization of CL-4, we next examined the effects of C-CPE–PSIF on cells of the human colon carcinoma line Caco-2, which express CL-4. When confluent, Caco-2 cells form a polarized cell monolayer with well-developed TJs; they are frequently used as a model of polarized cells.[25] We found that although CL-4 protein levels were greater in confluent than subconfluent cultures, C-CPE–PSIF was more toxic (47% cell death at 5 ng/mL) in preconfluent cells, which had fewer TJs. In contrast, cell death in confluent cells with well-developed TJs was not observed at doses as high as 10 ng/mL[22] (Fig. 1). To assess whether cellular polarity affects cell sensitivity to C-CPE–PSIF, we grew Caco-2 monolayers in culture chambers that allowed us to treat the apical and basolateral sides of the cells independently. Addition of C-CPE–PSIF to the basolateral compartment, but not the apical compartment, increased the amount of lactate dehydrogenase (a marker of cytotoxicity) that was released into the medium.[22] Therefore C-CPE–PSIF may specifically recognize cells in which cellular polarity is disrupted.

To evaluate the potential efficacy of a CL-4–targeting strategy, we investigated whether C-CPE–PSIF showed antitumor activity *in vivo*. We inoculated mice with 4T1 cells, a murine cell line frequently used as a spontaneous lung metastasis model,[26] then treated the mice with C-CPE–PSIF. C-CPE–PSIF significantly suppressed tumor growth (Fig. 2A) and lung metastasis (Fig. 2B) in 4T1-bearing mice. In addition, C-CPE–PSIF did not lead to decreases of body weight and to any apparent biochemical side effects in treated mice.[26] Together, these findings indicate that CL-targeting therapy may

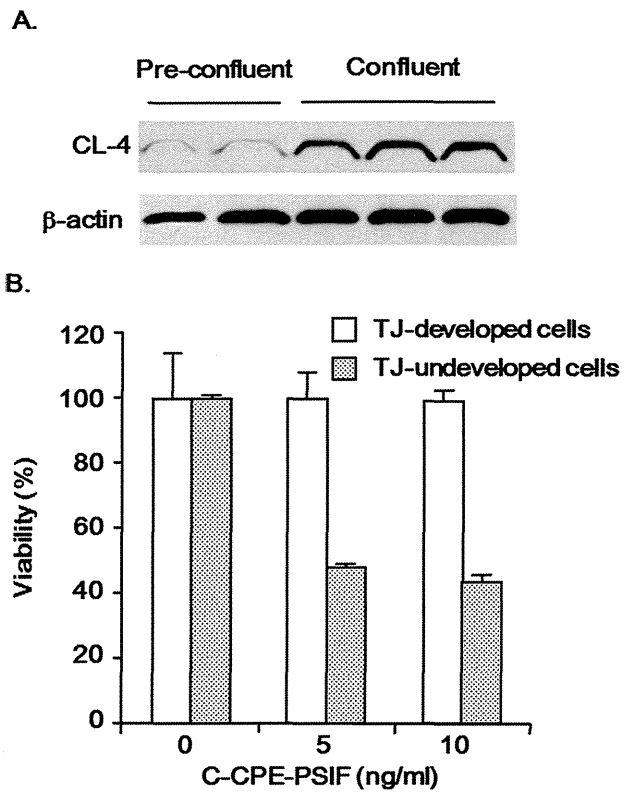

Fig. 1. Specificity of C-CPE–PSIF Cytotoxicity[22]

Caco-2 monolayers grown at confluency for 3 d were used as a source of cells with well-developed TJs (TJ-developed cells); in contrast, Caco-2 cells seeded at 10^4 cells/well in 96-well plates were used as a source of cells with immature TJs. (A) Lysates of these cell populations underwent SDS-PAGE followed by Western blotting with anti-CL-4 antibody. (B) In addition, cells were treated for 48 h with the indicated concentrations of C-CPE–PSIF, after which cell viability was measured by WST-8 assay.

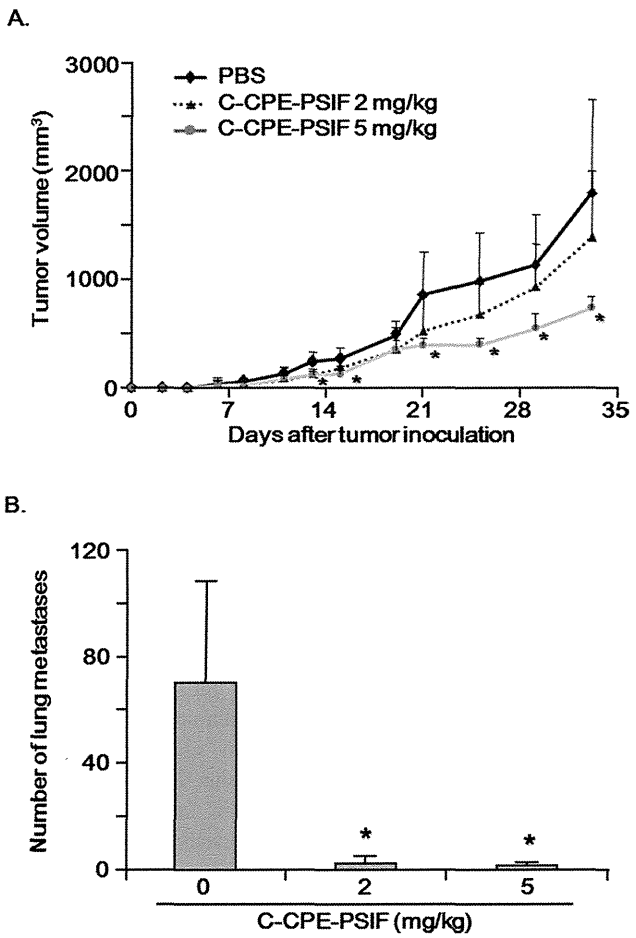

Fig. 2. Antitumor Activity of C-CPE–PSIF against 4T1 Murine Breast Cancer Cells[26]

4T1 cells (1×10^5) were inoculated intradermally into the right flanks of mice on day 0, after which C-CPE–PSIF was injected intravenously two or three times each week at the indicated doses. (A) Tumor volume was monitored. On day 35, the mice were euthanized, their lungs stained with India ink, and (B) spontaneous metastases counted. Data are shown as mean±S.D. (n=5). * Value significantly ($p<0.01$) different from that of the vehicle-treated group.

be a potent antitumor strategy.

3. TARGETING THE MUCOSA

Approximately 30 million people worldwide die from infectious diseases each year, thus demonstrating the dire importance of new methods to prevent infectious diseases. Vaccination against infectious diseases is a promising approach because it has few side effects and great preventative and therapeutic effects. Whereas parenteral vaccines injected into patients activate systemic immune responses, they fail to potentiate mucosal immune responses. Moreover, parenteral vaccines show poor patient compliance and poor preventive effects against invasion of pathologic microorganisms through the mucosa. In contrast, administration of mucosal vaccines is noninvasive, thus increasing patient compliance, and these agents potentiate both systemic and mucosal immune responses, thus preventing invasion of pathogens into the body as well as eliminating them and infected cells from the body. Therefore mucosal vaccination is an ideal strategy for protecting against infectious pathogens.[2,27]

On the other hand, mucosal administration of antigens

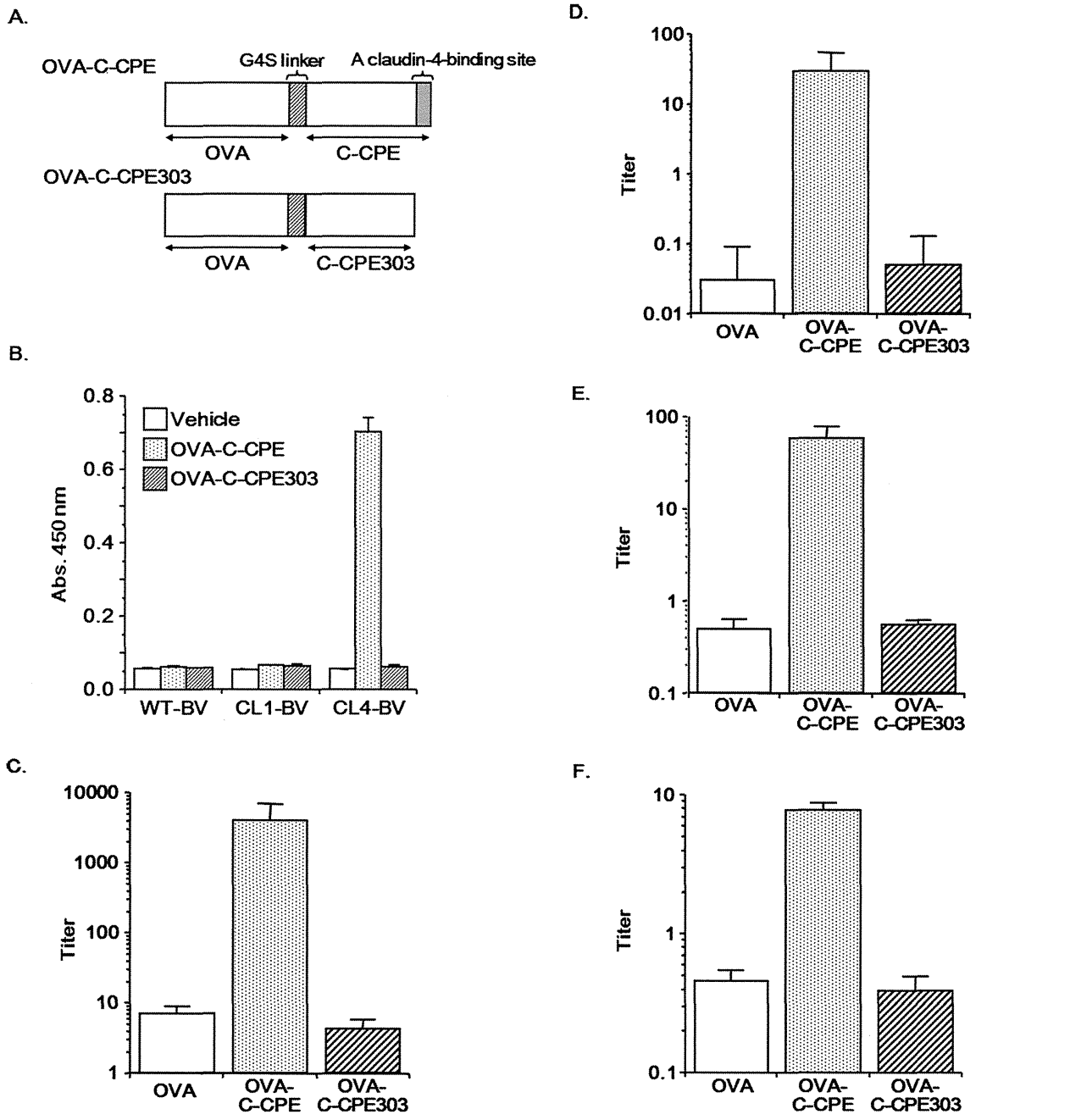

Fig. 3. Involvement of CL-4 in Immune Responses to OVA–C-CPE[34]

(A) Schematic illustration of OVA–C-CPE mutant. The construct in which the 16 C-terminal amino acids were deleted from C-CPE (that is, the C-CPE303 mutant) did not bind to CL-4. (B) Interaction of OVA–C-CPE303 with wild-type BV (WT-BV) or CL-1– or CL-4–displaying BV (CL1-BV, CL4-BV) was evaluated by ELISA. (C–F) Induction of immune responses by OVA–C-CPE or OVA–C-CPE303. Mice were immunized intranasally with OVA, OVA–C-CPE, or OVA–C-CPE303 (all doses equivalent to 5 μg OVA) once weekly for 3 weeks. Seven days after the last immunization, the levels of (C) serum IgG, (D) nasal IgA, (E) vaginal IgA, and (F) fecal IgA were measured by ELISA. Data are shown as mean±S.E.M. (n=4).

alone does not potentiate immune responses, and efficient delivery of antigens to mucosal immune tissues is essential for mucosal vaccination.[27–29] Mucosa-associated lymphoid tissues (MALTs) in the mucosal epithelium function as the first line of defense against pathogenic invasion *via* the epithelium by activating mucosal immune responses.[30,31] MALTs contain lymphocytes, M cells, T cells, B cells, and antigen-presenting cells (APCs) and are covered by follicle-associated epithelium (FAE). A specialized M-type epithelial cell in the FAE takes up antigen and presents it to the APCs, which are localized below the M cells, for processing.[32] Therefore ligands that target FAE or M cells may be useful for mucosal vaccination. In this regard, both FAE and M cells show considerable expression of CL-4,[19,33] suggesting the potential utility of CL-4–targeting in mucosal vaccination.

To evaluate whether a CL-4–targeting strategy would be effective for mucosal vaccination, we genetically fused C-CPE with ovalbumin (OVA), a popular model antigen for vaccination, to generate OVA–C-CPE. We also prepared OVA–C-CPE303, in which the CL-4-binding region was deleted (Fig. 3A). Like C-CPE, OVA–C-CPE bound to CL-4 but not CL-1, whereas OVA–C-CPE303 did not bind either CL (Fig. 3B). We then intranasally inoculated mice with OVA, OVA–C-CPE, or OVA–C-CPE303 once weekly for 3 weeks and measured OVA-specific serum immunoglobulin G (IgG), nasal IgA, vaginal IgA, and fecal IgA levels at 1 week after the last inoculation. All of these immune responses were activated in mice immunized with OVA–C-CPE but were attenuated in mice that received OVA–C-CPE303 (Figs. 3C–F). These findings suggest that CL-4–targeting is an effective antigen delivery system for mucosal vaccination.[34]

Antigen-specific immune responses are classified as Th1- and Th2-type responses.[35,36] To clarify the immune response profiles activated by CL-4–targeting, we investigated serum titers of IgG1 (a Th2 response) and IgG2a (a Th1 response) in mice nasally immunized with OVA–C-CPE or OVA–C-CPE303 and the production of interferon-γ (Th1-specific cytokine) and IL-13 (Th2-specific cytokine) from splenocytes isolated from those mice. Unlike OVA–C-CPE303, OVA–C-CPE markedly increased serum IgG1 and IgG2a titers and the production of interferon-γ and IL-13.[34] Therefore a CL-4–targeting vaccine may activate both Th1 and Th2 immune responses. To evaluate the immune responses induced by nasal vaccination with OVA–C-CPE, we investigated anti-tumor activity in mice bearing OVA-expressing thymoma cells. Mice were immunized with vehicle, OVA, a mixture of OVA and C-CPE, OVA–C-CPE, or OVA–C-CPE303 once weekly for 3 weeks. Seven days after the last immunization, the mice were inoculated subcutaneously with thymoma cells. Immunization with OVA–C-CPE—but not OVA alone, a mixture of OVA and C-CPE, or OVA-C-CPE303—suppressed tumor growth (Fig. 4). These findings suggest that mucosal vaccination using a CL-4–binding strategy protects against tumor challenge.[34]

4. DEVELOPING CL BINDERS

Recent progress in understanding the biochemical structure of TJs has provided new insights into CL-targeted drug development. In addition to their use as potent targets for cancer treatment and mucosal vaccination, CLs likely can be manipulated through the use of C-CPE to facilitate mucosal absorption of various drugs.[11,12] Although a key component of an effective mucosal drug-delivery system, the development of CL binders against the extracellular loop region of CLs has been largely unsuccessful because of the low antigenicity of CLs and the difficulty in preparing them as recombinant proteins.

In light of its efficacy as a ligand for cancer-targeting and mucosal vaccination, we used C-CPE as a prototype for new CL-binding agents. We used deletion analysis and alanine-scanning to map the functional domains of C-CPE.[37,38] We then prepared a phage library that contained phages displaying various C-CPE peptides in which individual functional amino acids had been randomly mutated to any of the 20 amino acids.[39]

A novel type of protein expression system using budded

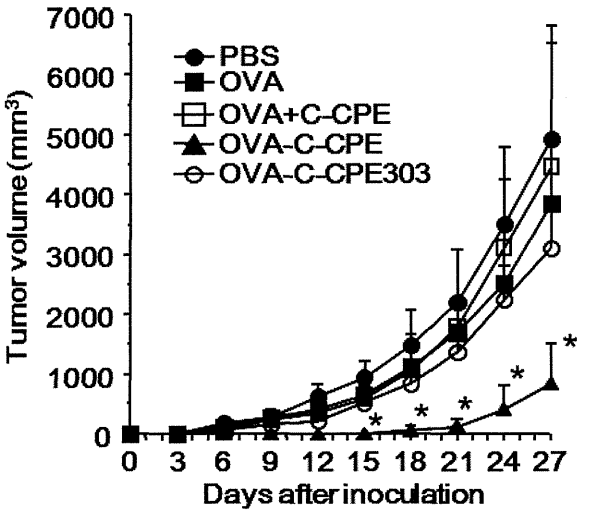

Fig. 4. Antitumor Activity Induced by Immunization with OVA–C-CPE in an EG7 Cancer Model, OVA-Expressing Thymoma[34]

Mice were nasally immunized with vehicle, OVA, a mixture of OVA and C-CPE, OVA–C-CPE, or OVA–C-CPE303 (all doses equivalent to 5 μg OVA) once weekly for 3 weeks. Seven days after the last immunization, the mice were injected subcutaneously in the right back with EG7 cells (1×10^6). Tumor volumes were calculated. Data are given as mean±S.D. (n=4). * Value significantly ($p<0.05$) different from that of the vehicle-immunized group.

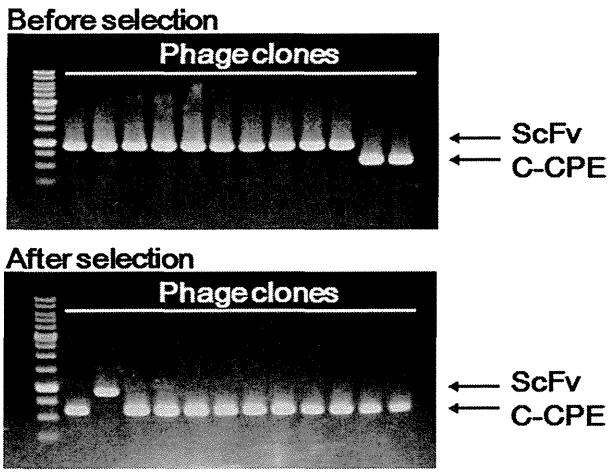

Fig. 5. Selection of C-CPE–Displaying Phage Using CL-4–BV System[39]

A mixture of scFv–phage and C-CPE–phage (ratio, 2:10) was incubated in CL4–BV-coated immunotubes and the bound phages recovered. Phage clones were identified by PCR amplification followed by agarose gel electrophoresis (sizes of putative PCR products: scFv, 856 bp; C-CPE, 523 bp). Upper panel, before selection using CL4–BV-coated immunotubes; lower panel, after selection.

baculovirus (BV) has been developed recently, in which membrane proteins are displayed in their active form.[40,41] Consequently, we investigated whether CL-displaying BV could be used to screen for CL-binding peptides. In this regard, CL-4–displaying BV interacted with C-CPE but not C-CPE303.[39] We then used CL-4–displaying BV to enrich for C-CPE–phages from a mixture containing scFv–phages and C-CPE–phages[39] (Fig. 5). These findings indicate that CL-displaying BV may be a useful screening system for identifying CL-binding peptides.

Like CL-4, CL-1 is a promising target for modulating mucosal and epidermal barriers, preventing infection by hepatitis C virus, and targeting cancer cells.[9,15,42,43] Accordingly, we used a mutant C-CPE phage library and CL-1–displaying BV to screen for peptides with CL-1–binding activity. After three rounds of screening, we isolated a single promising CL-1–binding candidate, m19, which interacted with both CL-1– and CL-4–displaying BV. Subsequent flow cytometry revealed that m19 binds to cells that express CL-1, CL-2, CL-4, or CL-5 (Fig. 6). Therefore m19 may be the first broadly specific CL

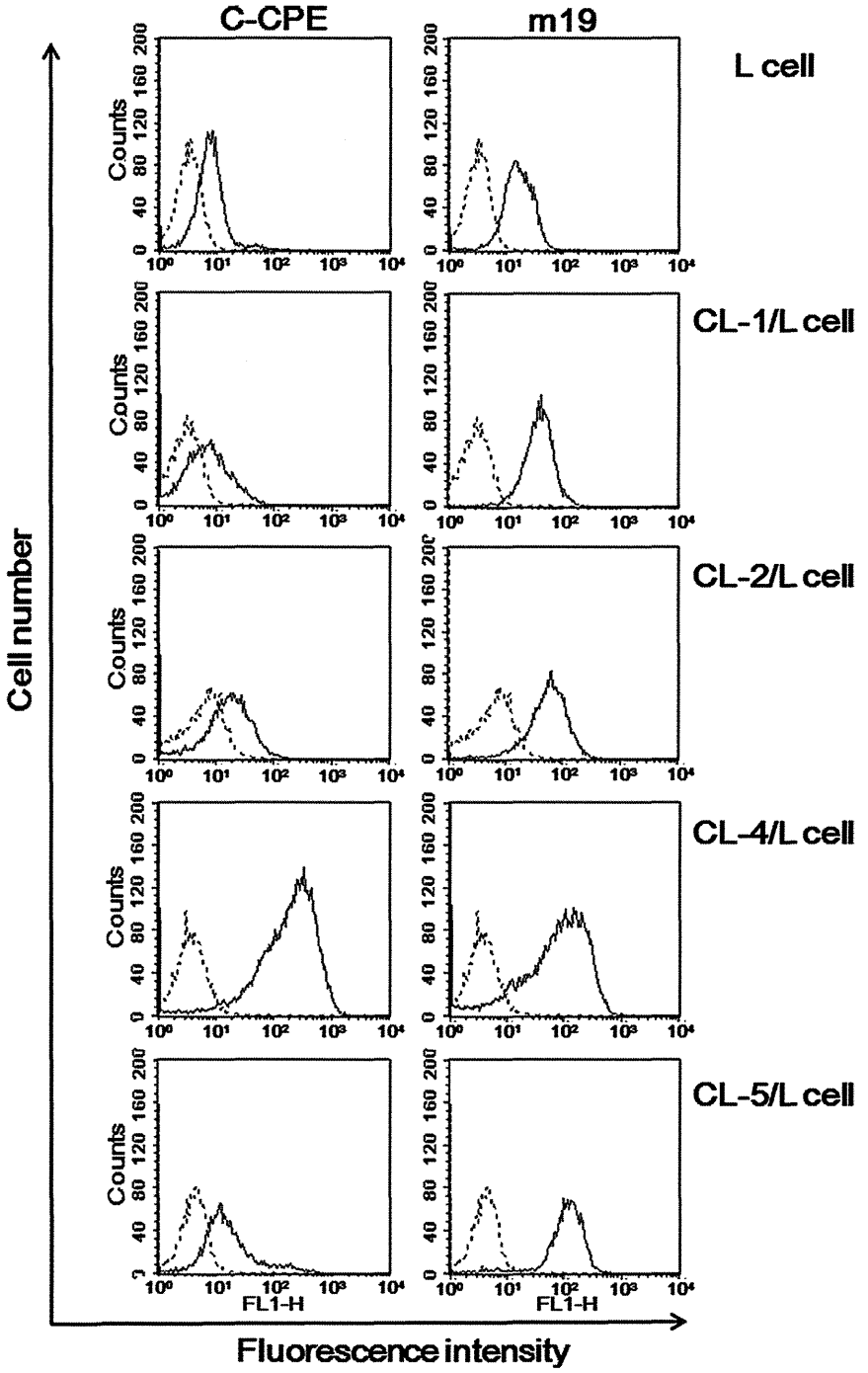

Fig. 6. Flow Cytometric Analysis of Interaction between m19 and CL-Expressing L Cells[44]

CL-expressing L cells were treated with C-CPE or m19; labeled secondary antibodies were used to visualize bound C-CPE or m19 through flow cytometry. Solid histograms indicate the level of reactivity of C-CPE or m19; dotted histograms indicate background binding of the anti-His tag and FITC-labeled antibodies without C-CPE or m19.

binder.[44]

Because understanding the mode of action of m19 would yield information useful in the development of CL binders, we performed X-ray structural analysis to determine the structures and electrostatic surface maps of m19 and C-CPE. Whereas m19 and C-CPE were structurally similar, the electrostatic maps of their CL-binding regions were greatly different. The binding region of C-CPE is negatively charged, whereas that of m19 is positively charged.[44] Analysis of a series of chimeras revealed that sensitivity to CPE was determined by the region from Asn149 to Met160 in CLs (that is, the CPE sensitivity-related region; CPE-SR).[45] The isoelectric point (p*I*) values of CPE-SRs in CL-4, CL-1, CL-2, and CL-5 were revealed as 9.70, 4.18, 4.18, and 4.18, respectively. Taken together, these findings suggest that varying the electrostatic charge of the CL-binding region of C-CPE may be a useful method to create CL binders.

5. PERSPECTIVES OF CL-TARGETED DRUG DELIVERY

Applications of C-CPE and its derivatives are limited because of their origins in enterotoxin. Indeed, repeated administration of C-CPE induced production of antibodies in mice.[46] Therefore development of biocompatible CL binders and ligands such as chemicals, peptides, and antibodies is crucial for their application as therapeutics.

Two groups have developed anti-CL antibodies recently. An antibody directed against the extracellular loop region of CL-4 demonstrated antibody-dependent cellular cytotoxicity and *in vivo* antitumor activity.[47] Another group created anti-CL-1 antibodies that prevented the infection of human hepatocytes by hepatitis C virus.[48] Although these successes will encourage further development of CL antibodies, the high costs associated with this process likely will limit the clinical application of these reagents to the treatment of widespread diseases such as cancer and hepatitis C. In addition, CL-binding chemicals or peptides must be created to capitalize on the capacity for noninvasive administration and drug delivery to peripheral and central neurons through modulation of CLs. To this end, the three-dimensional structures of CLs need to be determined, and the process of developing antibodies to CLs may yield insights into their solubilization and crystallization. Furthermore, CL-displaying BV may be a valuable tool for screening of candidate CL binders, as mentioned previously.[39]

The development of CL-targeting systems is in its very early stages, and additional applications of CL-targeted drug delivery remain to be proposed. We believe that the current problems regarding the development of CL binders will be overcome and that the promise of the clinical value of CL-targeted pharmaceutical therapies will be realized.

Acknowledgements This work was supported in part by Grants-in-Aid for Scientific Research from the Ministry of Education, Culture, Sports, Science and Technology of Japan (21689006, 24390042) and by Health and Labor Sciences Research Grants from the Ministry of Health, Labour and Welfare of Japan.

REFERENCES

1) Wodarz A, Näthke I. Cell polarity in development and cancer. *Nat. Cell Biol.*, **9**, 1016–1024 (2007).
2) Kunisawa J, Nochi T, Kiyono H. Immunological commonalities and distinctions between airway and digestive immunity. *Trends Immunol.*, **29**, 505–513 (2008).
3) Powell DW. Barrier function of epithelia. *Am. J. Physiol.*, **241**, G275–G288 (1981).
4) Windsor E, Cronheim GE. Gastro-intestinal absorption of heparin and synthetic heparinoids. *Nature*, **190**, 263–264 (1961).
5) Schneeberger EE, Lynch RD. The tight junction: a multifunctional complex. *Am. J. Physiol. Cell Physiol.*, **286**, C1213–C1228 (2004).
6) Higashi T, Tokuda S, Kitajiri SI, Masuda S, Nakamura H, Oda Y, Furuse M. Analysis of the angulin family consisting of LSR, ILDR1 and ILDR2: tricellulin recruitment, epithelial barrier function and implication in deafness pathogenesis. *J. Cell Sci.*, (2012), in press.
7) Masuda S, Oda Y, Sasaki H, Ikenouchi J, Higashi T, Akashi M, Nishi E, Furuse M. LSR defines cell corners for tricellular tight junction formation in epithelial cells. *J. Cell Sci.*, **124**, 548–555 (2011).
8) Ikenouchi J, Furuse M, Furuse K, Sasaki H, Tsukita S, Tsukita S. Tricellulin constitutes a novel barrier at tricellular contacts of epithelial cells. *J. Cell Biol.*, **171**, 939–945 (2005).
9) Furuse M, Hata M, Furuse K, Yoshida Y, Haratake A, Sugitani Y, Noda T, Kubo A, Tsukita S. Claudin-based tight junctions are crucial for the mammalian epidermal barrier: a lesson from claudin-1-deficient mice. *J. Cell Biol.*, **156**, 1099–1111 (2002).
10) Hackel D, Krug SM, Sauer RS, Mousa SA, Böcker A, Pflücke D, Wrede EJ, Kistner K, Hoffmann T, Niedermirtl B, Sommer C, Bloch L, Huber O, Blasig IE, Amasheh S, Reeh PW, Fromm M, Brack A, Rittner HL. Transient opening of the perineurial barrier for analgesic drug delivery. *Proc. Natl. Acad. Sci. U.S.A.*, **109**, E2018–E2027 (2012).
11) Nitta T, Hata M, Gotoh S, Seo Y, Sasaki H, Hashimoto N, Furuse M, Tsukita S. Size-selective loosening of the blood–brain barrier in claudin-5-deficient mice. *J. Cell Biol.*, **161**, 653–660 (2003).
12) Kondoh M, Masuyama A, Takahashi A, Asano N, Mizuguchi H, Koizumi N, Fujii M, Hayakawa T, Horiguchi Y, Watanbe Y. A novel strategy for the enhancement of drug absorption using a claudin modulator. *Mol. Pharmacol.*, **67**, 749–756 (2005).
13) Uchida H, Kondoh M, Hanada T, Takahashi A, Hamakubo T, Yagi K. A claudin-4 modulator enhances the mucosal absorption of a biologically active peptide. *Biochem. Pharmacol.*, **79**, 1437–1444 (2010).
14) Kominsky SL. Claudins: emerging targets for cancer therapy. *Expert Rev. Mol. Med.*, **8**, 1–11 (2006).
15) Morin PJ. Claudin proteins in human cancer: promising new targets for diagnosis and therapy. *Cancer Res.*, **65**, 9603–9606 (2005).
16) Kominsky SL, Tyler B, Sosnowski J, Brady K, Doucet M, Nell D, Smedley JG 3rd, McClane B, Brem H, Sukumar S. *Clostridium perfringens* enterotoxin as a novel-targeted therapeutic for brain metastasis. *Cancer Res.*, **67**, 7977–7982 (2007).
17) Michl P, Buchholz M, Rolke M, Kunsch S, Löhr M, McClane B, Tsukita S, Leder G, Adler G, Gress TM. Claudin-4: a new target for pancreatic cancer treatment using *Clostridium perfringens* enterotoxin. *Gastroenterology*, **121**, 678–684 (2001).
18) Santin AD, Cané S, Bellone S, Palmieri M, Siegel ER, Thomas M, Roman JJ, Burnett A, Cannon MJ, Pecorelli S. Treatment of chemotherapy-resistant human ovarian cancer xenografts in C.B-17/SCID mice by intraperitoneal administration of *Clostridium perfringens* enterotoxin. *Cancer Res.*, **65**, 4334–4342 (2005).
19) Tamagawa H, Takahashi I, Furuse M, Yoshitake-Kitano Y, Tsukita S, Ito T, Matsuda H, Kiyono H. Characteristics of claudin expression in follicle-associated epithelium of Peyer's patches: preferential localization of claudin-4 at the apex of the dome region. *Lab. In-*

vest., **83**, 1045–1053 (2003).
20) Jemal A, Siegel R, Ward E, Hao Y, Xu J, Murray T, Thun MJ. Cancer statistics, 2008. *CA Cancer J. Clin.*, **58**, 71–96 (2008).
21) Ebihara C, Kondoh M, Hasuike N, Harada M, Mizuguchi H, Horiguchi Y, Fujii M, Watanabe Y. Preparation of a claudin-targeting molecule using a C-terminal fragment of *Clostridium perfringens* enterotoxin. *J. Pharmacol. Exp. Ther.*, **316**, 255–260 (2006).
22) Saeki R, Kondoh M, Kakutani H, Tsunoda S, Mochizuki Y, Hamakubo T, Tsutsumi Y, Horiguchi Y, Yagi K. A novel tumor-targeted therapy using a claudin-4-targeting molecule. *Mol. Pharmacol.*, **76**, 918–926 (2009).
23) Kreitman RJ, Pastan I. Immunotoxins in the treatment of hematologic malignancies. *Curr. Drug Targets*, **7**, 1301–1311 (2006).
24) Ogata M, Chaudhary VK, Pastan I, FitzGerald DJ. Processing of *Pseudomonas* exotoxin by a cellular protease results in the generation of a 37,000-Da toxin fragment that is translocated to the cytosol. *J. Biol. Chem.*, **265**, 20678–20685 (1990).
25) Meunier V, Bourrie M, Berger Y, Fabre G. The human intestinal epithelial cell line Caco-2; pharmacological and pharmacokinetic applications. *Cell Biol. Toxicol.*, **11**, 187–194 (1995).
26) Saeki R, Kondoh M, Kakutani H, Matsuhisa K, Takahashi A, Suzuki H, Kakamu Y, Watari A, Yagi K. A claudin-targeting molecule as an inhibitor of tumor metastasis. *J. Pharmacol. Exp. Ther.*, **334**, 576–582 (2010).
27) Boyaka PN, Marinaro M, Vancott JL, Takahashi I, Fujihashi K, Yamamoto M, van Ginkel FW, Jackson RJ, Kiyono H, McGhee JR. Strategies for mucosal vaccine development. *Am. J. Trop. Med. Hyg.*, **60** (Suppl), 35–45 (1999).
28) Cárdenas-Freytag L, Cheng E, Mirza A. New approaches to mucosal immunization. *Adv. Exp. Med. Biol.*, **473**, 319–337 (1999).
29) Michels KB, zur Hausen H. HPV vaccine for all. *Lancet*, **374**, 268–270 (2009).
30) Kiyono H, Fukuyama S. NALT- *versus* Peyer's-patch-mediated mucosal immunity. *Nat. Rev. Immunol.*, **4**, 699–710 (2004).
31) Kunisawa J, Fukuyama S, Kiyono H. Mucosa-associated lymphoid tissues in the aerodigestive tract: their shared and divergent traits and their importance to the orchestration of the mucosal immune system. *Curr. Mol. Med.*, **5**, 557–572 (2005).
32) Owen RL, Piazza AJ, Ermak TH. Ultrastructural and cytoarchitectural features of lymphoreticular organs in the colon and rectum of adult BALB/c mice. *Am. J. Anat.*, **190**, 10–18 (1991).
33) Ling J, Liao H, Clark R, Wong MS, Lo DD. Structural constraints for the binding of short peptides to claudin-4 revealed by surface plasmon resonance. *J. Biol. Chem.*, **283**, 30585–30595 (2008).
34) Kakutani H, Kondoh M, Fukasaka M, Suzuki H, Hamakubo T, Yagi K. Mucosal vaccination using claudin-4-targeting. *Biomaterials*, **31**, 5463–5471 (2010).
35) Yamamoto S, Kiyono H, Yamamoto M, Imaoka K, Fujihashi K, Van Ginkel FW, Noda M, Takeda Y, McGhee JR. A nontoxic mutant of cholera toxin elicits Th2-type responses for enhanced mucosal immunity. *Proc. Natl. Acad. Sci. U.S.A.*, **94**, 5267–5272 (1997).
36) Yanagita M, Hiroi T, Kitagaki N, Hamada S, Ito HO, Shimauchi H, Murakami S, Okada H, Kiyono H. Nasopharyngeal-associated lymphoreticular tissue (NALT) immunity: fimbriae-specific Th1 and Th2 cell-regulated IgA responses for the inhibition of bacterial attachment to epithelial cells and subsequent inflammatory cytokine production. *J. Immunol.*, **162**, 3559–3565 (1999).
37) Takahashi A, Kondoh M, Masuyama A, Fujii M, Mizuguchi H, Horiguchi Y, Watanabe Y. Role of C-terminal regions of the C-terminal fragment of *Clostridium perfringens* enterotoxin in its interaction with claudin-4. *J. Control. Release*, **108**, 56–62 (2005).
38) Takahashi A, Komiya E, Kakutani H, Yoshida T, Fujii M, Horiguchi Y, Mizuguchi H, Tsutsumi Y, Tsunoda S, Koizumi N, Isoda K, Yagi K, Watanabe Y, Kondoh M. Domain mapping of a claudin-4 modulator, the C-terminal region of C-terminal fragment of *Clostridium perfringens* enterotoxin, by site-directed mutagenesis. *Biochem. Pharmacol.*, **75**, 1639–1648 (2008).
39) Kakutani H, Takahashi A, Kondoh M, Saito Y, Yamaura T, Sakihama T, Hamakubo T, Yagi K. A novel screening system for claudin binder using baculoviral display. *PLoS ONE*, **6**, e16611 (2011).
40) Loisel TP, Ansanay H, St-Onge S, Gay B, Boulanger P, Strosberg AD, Marullo S, Bouvier M. Recovery of homogeneous and functional beta 2-adrenergic receptors from extracellular baculovirus particles. *Nat. Biotechnol.*, **15**, 1300–1304 (1997).
41) Sakihama T, Masuda K, Sato T, Doi T, Kodama T, Hamakubo T. Functional reconstitution of G-protein-coupled receptor-mediated adenylyl cyclase activation by a baculoviral co-display system. *J. Biotechnol.*, **135**, 28–33 (2008).
42) Evans MJ, von Hahn T, Tscherne DM, Syder AJ, Panis M, Wölk B, Hatziioannou T, McKeating JA, Bieniasz PD, Rice CM. Claudin-1 is a hepatitis C virus co-receptor required for a late step in entry. *Nature*, **446**, 801–805 (2007).
43) Amasheh M, Grotjohann I, Amasheh S, Fromm A, Söderholm JD, Zeitz M, Fromm M, Schulzke JD. Regulation of mucosal structure and barrier function in rat colon exposed to tumor necrosis factor alpha and interferon gamma *in vitro*: a novel model for studying the pathomechanisms of inflammatory bowel disease cytokines. *Scand. J. Gastroenterol.*, **44**, 1226–1235 (2009).
44) Takahashi A, Saito Y, Kondoh M, Matsushita K, Krug SM, Suzuki H, Tsujino H, Li X, Aoyama H, Matsuhisa K, Uno T, Fromm M, Hamakubo T, Yagi K. Creation and biochemical analysis of a broad-specific claudin binder. *Biomaterials*, **33**, 3464–3474 (2012).
45) Kimura J, Abe H, Kamitani S, Toshima H, Fukui A, Miyake M, Kamata Y, Sugita-Konishi Y, Yamamoto S, Horiguchi Y. *Clostridium perfringens* enterotoxin interacts with claudins *via* electrostatic attraction. *J. Biol. Chem.*, **285**, 401–408 (2010).
46) Suzuki H, Kondoh M, Li X, Takahashi A, Matsuhisa K, Matsushita K, Kakamu Y, Yamane S, Kodaka M, Isoda K, Yagi K. A toxicological evaluation of a claudin modulator, the C-terminal fragment of *Clostridium perfringens* enterotoxin, in mice. *Pharmazie*, **66**, 543–546 (2011).
47) Suzuki M, Kato-Nakano M, Kawamoto S, Furuya A, Abe Y, Misaka H, Kimoto N, Nakamura K, Ohta S, Ando H. Therapeutic antitumor efficacy of monoclonal antibody against claudin-4 for pancreatic and ovarian cancers. *Cancer Sci.*, **100**, 1623–1630 (2009).
48) Fofana I, Krieger SE, Grunert F, Glauben S, Xiao F, Fafi-Kremer S, Soulier E, Royer C, Thumann C, Mee CJ, McKeating JA, Dragic T, Pessaux P, Stoll-Keller F, Schuster C, Thompson J, Baumert TF. Monoclonal anti-claudin 1 antibodies prevent hepatitis C virus infection of primary human hepatocytes. *Gastroenterology*, **139**, 953–964, 964, e1–e4 (2010).

Nanoscale Research Letters
a SpringerOpen Journal

NANO EXPRESS Open Access

Acute and chronic nephrotoxicity of platinum nanoparticles in mice

Yoshiaki Yamagishi[1], Akihiro Watari[1*], Yuya Hayata[1], Xiangru Li[1], Masuo Kondoh[1], Yasuo Yoshioka[2], Yasuo Tsutsumi[2] and Kiyohito Yagi[1]

Abstract

Platinum nanoparticles are being utilized in various industrial applications, including in catalysis, cosmetics, and dietary supplements. Although reducing the size of the nanoparticles improves the physicochemical properties and provides useful performance characteristics, the safety of the material remains a major concern. The aim of the present study was to evaluate the biological effects of platinum particles less than 1 nm in size (snPt1). In mice administered with a single intravenous dose of snPt1, histological analysis revealed necrosis of tubular epithelial cells and urinary casts in the kidney, without obvious toxic effects in the lung, spleen, and heart. These mice exhibited dose-dependent elevation of blood urea nitrogen, an indicator of kidney damage. Direct application of snPt1 to *in vitro* cultures of renal cells induced significant cytotoxicity. In mice administered for 4 weeks with twice-weekly intraperitoneal snPt1, histological analysis of the kidney revealed urinary casts, tubular atrophy, and inflammatory cell accumulation. Notably, these toxic effects were not observed in mice injected with 8-nm platinum particles, either by single- or multiple-dose administration. Our findings suggest that exposure to platinum particles of less than 1 nm in size may induce nephrotoxicity and disrupt some kidney functions. However, this toxicity may be reduced by increasing the nanoparticle size.

Keywords: Nanosized materials; Platinum particles; Kidney; Nephrotoxicity; Safety evaluation

Background

Nanomaterials have been developed and used as innovative materials in a wide range of industrial fields, including electronics, medicine, food, clothing, and cosmetics; these reagents are expected to provide significant benefits to humans. Nanomaterials are defined as substances that have at least one dimension size below 100 nm. The reduced size provides novel physicochemical properties, including increased thermal electrical conductivity, durability, and strength [1-3]. Although these characteristics may yield improved performance and novel functions, several reports have suggested that various types of nanomaterials, such as carbon nanotubes, titanium dioxide, fullerenes, quantum dots, and silica, exhibit harmful biological effects [4-12]. Additionally, some reports have shown that the characteristics of nanoparticles (e.g., size and surface features) can affect their biological and pathological actions [10,13-16]. Therefore, evaluation of the potential health risks attributable to nanomaterials is indispensable for the safe handling and use of these materials. However, little information is available regarding the safety evaluation of materials less than 1 nm in size.

Platinum nanoparticles have been utilized in a number of manufacturing applications, including catalysis, cosmetics manufacturing, and the processing of dietary supplements. As products using platinum nanoparticles become more familiar in our daily lives, the chances of exposure to platinum nanoparticles are increasing, as are concerns about unanticipated harmful biological effects of these materials [17,18]. In fact, there are some reports that platinum nanoparticles can induce inflammation in mice or impair the integrity of DNA [19,20]. On the other hand, platinum nanoparticles have antioxidant activity and inhibit pulmonary inflammation (e.g., as caused by exposure to cigarette smoke) [21-23]. These reports indicate that the biological effects of platinum nanoparticles remain poorly defined; the biological safety of sub-nanosized platinum particles (those of less

* Correspondence: akihiro@phs.osaka-u.ac.jp
[1]Laboratories of Bio-Functional Molecular Chemistry, Graduate School of Pharmaceutical Sciences, Osaka University, Suita, Osaka 565-0871, Japan
Full list of author information is available at the end of the article

than 1 nm in size; snPt1) remains unknown. Recently, we reported that snPt1 can induce hepatotoxicity [24]. However, the biological effects of snPt1 on other organs remain unclear. In this study, we evaluated the effect of snPt1 on tissues after single- and multi-dose administration in mice. In addition, we investigated the relationship between platinum particle size and biological response by also testing platinum particles of 8 nm in size (snPt8).

Methods

Platinum particles

Platinum particles with nominal mean diameters of less than 1 nm (snPt1) and 8 nm (snPt8) were purchased from Polytech & Net GmbH (Rostock, Germany). The particle sizes were confirmed using a Zetasizer Nano-ZS (Malvern Instruments, Malvern, UK). The particles were stocked as 5 mg/ml aqueous suspensions. The stock solutions were suspended using a vortex mixer before use. Other reagents used in this study were of research grade.

Animals

BALB/c and C57BL/6 male mice were obtained from Shimizu Laboratory Supplies Co., Ltd. (Kyoto, Japan) and were housed in an environmentally controlled room at 23°C ± 1.5°C with a 12-h light/12-h dark cycle. Mice had *ad libitum* access to water and commercial chow (Type MF, Oriental Yeast, Tokyo, Japan). BALB/c mice were injected intravenously with snPt1 or snPt8 at 5 to 20 mg/kg body weight. C57BL/6 mice were injected intraperitoneally with snPt1 or snPt8 at 10 mg/kg body weight, or with an equivalent volume of vehicle (water). At 24 h after the injection of the vehicle or test article, the kidney and liver were collected. For testing the chronic effects of platinum particles, C57BL/6 mice were injected intraperitoneally with snPt1 or snPt8 at 10 mg/kg body weight, or with an equivalent volume of vehicle (water). Intraperitoneal doses were administered as twice-weekly injections for 4 weeks. At 72 h after the last injection of vehicle or test article, the kidney and liver were collected. All experimental protocols conformed to the ethical guidelines of the Graduate School of Pharmaceutical Sciences at Osaka University.

Histological analysis

For animals dosed intravenously with snPt1 or snPt8, the kidney, spleen, lung, heart, and liver were removed at 24 h post-injection and fixed with 4% paraformaldehyde. For

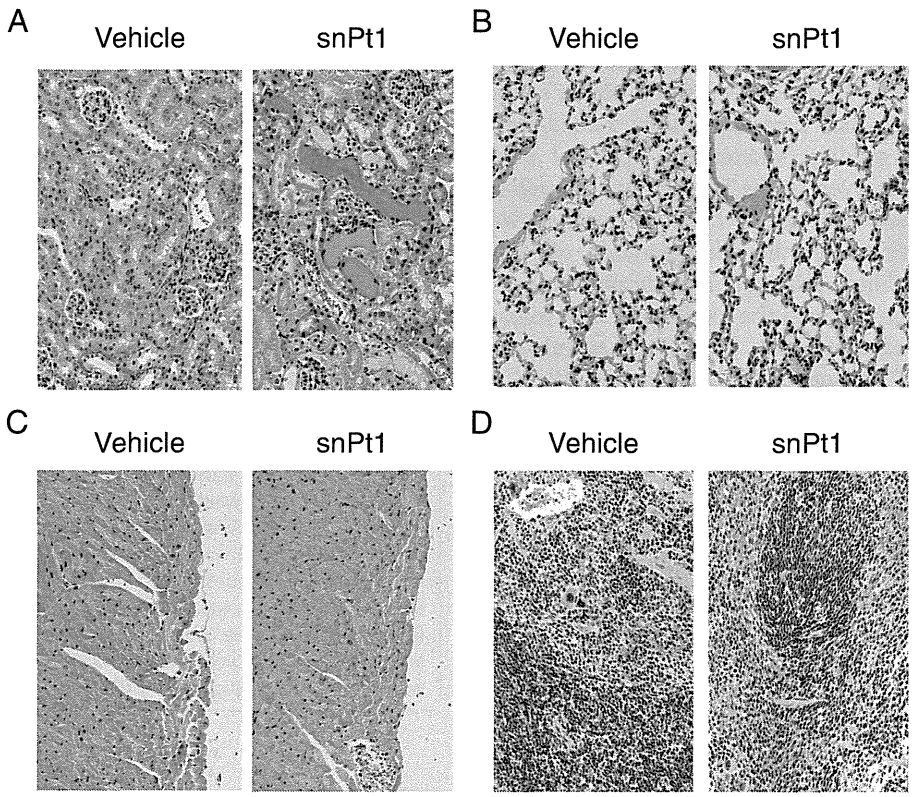

Figure 1 Histological analysis of the organs in snPt1-treated mice. Vehicle (water) or snPt1 (15 mg/kg) was administered intravenously to mice. At 24 h after administration, the kidney **(A)**, lung **(B)**, heart **(C)**, and spleen **(D)** were collected and fixed with 4% paraformaldehyde. Tissue sections were stained with hematoxylin and eosin and observed microscopically.